Available online at www.sciencedirect.com
ScienceDirect
Geochimica et Cosmochimica Acta 71 (2007) 942–960
Geochimica
www.elsevier.com/locate/gca

Rare earth element and Pb isotope variations in a 52 kyr peat core from Lynch's Crater (NE Queensland, Australia): Proxy development and application to paleoclimate in the Southern Hemisphere

M.E. Kylander [a,b,*], J. Muller [c], R.A.J. Wüst [c], K. Gallagher [a], R. Garcia-Sanchez [b], B.J. Coles [a,b], D.J. Weiss [a,b,*]

[a] Department of Earth Science and Engineering, Imperial College London, London SW7 2AZ, UK
[b] Department of Mineralogy, The Natural History Museum London, London SW7 5BD, UK
[c] School of Earth Sciences, James Cook University, Townsville, 4811 Qld, Australia

Received 5 January 2006; accepted in revised form 23 October 2006

Abstract

Accurate prediction of future climate scenarios is contingent on our understanding of past and present climate mechanisms. This is done in part through the reconstruction of historical climate changes using proxy records from terrestrial and marine archives. Terrestrial archives covering the Holocene and late Pleistocene are limited, most acutely in the Southern Hemisphere. Here, Rare earth elements (REE) and Pb isotopes are developed as inorganic geochemical proxies of mineral dust source changes and, by extension, climate change. Using a peat core from Lynch's Crater in NE Queensland, Australia, we present the first long-term (c. 52 kyr) terrestrial record of atmospheric REE and Pb deposition (with the exception of four wet events which represent periods of erosion from the crater itself) in the Southern Hemisphere covering both glacial and interglacial times. Based on a combination of correlation analyses, Al and Ti normalised profiles and elemental patterns, we establish REE are immobile within the peat deposit and not subject to significant post depositional diagenetic changes (important particularly for Ce). This is vital as REE can be mobile under acid and organic rich conditions like those that can occur during the development of a peat deposit. The volcanic provinces of eastern Australia have characteristic Eu anomaly signatures, which allowed their use in a novel way to detect changes in dust source to Lynch's Crater. Between 41,095 and 52,505 BP the deposit was under the influence of dust carried by long distance transport (>1500 km) from SE Australia. From 8525 to 40,815 BP regional sources (100–1500 km) dominated the deposited signals while between 1740 and 8390 BP the dust signal was controlled by local sources (<100 km). These findings were also confirmed by Pb isotope data. Changepoint modelling refined the timing of these changes in dust source, recognizing concurrent shifts in our tracing tools ($(Eu/Eu^*)_{PAAS}$ and $^{206}Pb/^{207}Pb$). These changepoints were then compared to other palaeoenvironmental records (pollen, lake levels and dune building) from eastern Australia and found to be similar. Our results demonstrate that REE and Pb isotopes are effective tools for tracing past changes in atmospheric dust sources and to the study of climate change using minerotrophic peat deposits.

1. Introduction

Mineral dusts play an important part in the earth's climate system affecting radiation budgets, influencing the chemical composition of the atmosphere and supplying nutrients to terrestrial and marine ecosystems (Kohfeld and Harrison, 2001). Records of dust deposition are pivotal as they identify changes in fluxes and sources of eolian material. Fluctuations in dust can indicate more humid or arid conditions in different locations and is linked to changes in wet/dry deposition, temperature, vegetation cover and/or wind regimes. In this context, one region of

* Corresponding authors.
E-mail addresses: malin.kylander@gmail.com (M.E. Kylander), d.weiss@imperial.ac.uk (D.J. Weiss).

0016-7037/$ - see front matter © 2006 Elsevier Inc. All rights reserved.
doi:10.1016/j.gca.2006.10.018

particular paleoclimatic interest is Australia, the most significant modern dust source area in the Southern Hemisphere and the most arid continent on earth (McTainsh, 1989; Rea, 1994). In this work a peat core from Lynch's Crater in NE Queensland, Australia is used to develop novel inorganic geochemical proxies of dust source change. Lynch's Crater has been used extensively in climate reconstructions, particularly pollen based ones (e.g., Kershaw, 1974, 1994; Turney et al., 2004), providing an independent means by which to assess these new proxies.

Peatlands are unique terrestrial geochemical archives, capturing changes in atmospheric deposition of trace metals and dusts over time. These high-resolution records can cover extended time periods with some peat deposits dating back to the late Pleistocene. This has provided many valuable records of anthropogenic heavy metal pollution in the Northern Hemisphere (Lee and Tallis, 1973; Brännvall et al., 1997; Weiss et al., 1999; Klaminder et al., 2003; Shotyk et al., 2003). As yet only a few peat cores have been used to reconstruct climate change, despite the obvious potential. For example, peat cores have identified a Younger Dryas like event in SE Asia (Weiss et al., 2002); cold and warm periods in Southern Europe (Martínez Cortizas et al., 1999); and the impact of Saharan drying in Southern Europe (Kylander et al., 2005).

The Rare earth elements (REE) form a coherent group (from La to Lu) whose properties show ordered responses across the series during chemical and physical processes. During crustal weathering the chemical composition of the source rock is inherited and REE data, both isotopic and elemental, have been used in paleoclimatic studies e.g., to trace dust deposited in the South Atlantic Ocean during the Quaternary to source regions in South America (Gaiero et al., 2004). Within the REE suite however, Eu and Ce can develop anomalies (i.e., show different behaviour from neighbouring elements). Europium can be reduced to Eu^{2+} during high temperature igneous processes (>250 °C), allowing for greater substitution and enrichment of Eu in rock forming minerals, particularly plagioclase (Wilson, 2000). The redox environment similarly affects Ce, but anomalies are generated under low temperature oxidizing conditions. Eu anomalies are generally considered to be inherited from source rocks while Ce anomalies are generated post depositionally (Taylor and McLennan, 1985; McLennan, 1989).

Examination of REE in peats has to date been limited and focussed on time frames much shorter than those considered here (Ylirukanen and Lehto, 1995; Shotyk et al., 2001; Akagi et al., 2002; Krachler et al., 2003; Aubert et al., 2006). The signals archived at Lynch's Crater are a reflection of both source rock and soil weathering and related controls on dust deposition (i.e., external factors) as well as post depositional processes occurring within the mire (i.e., internal factors). Attempts to reconstruct changes in dust are dependent on determining the significance of the latter. In particular, REE mobility within the profile, leaching of REE from deposited minerals and changes in the redox sensitive element Ce, are of concern.

Using both elemental concentration and Pb isotope data analysed in a 13 m peat core collected from Lynch's Crater, NE Queensland, Australia our main objectives were to (i) explore REE behaviour, particularly in terms of post depositional changes in the organic rich, water logged, variable pH environment of the mire; (ii) develop REE, supported by Pb isotope data, as a tool to identify changes in dust source; and (iii) apply changes in dust source as a proxy of climate change as recorded at Lynch's Crater over the last 52 kyr. This is the only long-term peat core from the Southern Hemisphere, covering both glacial and interglacial periods, to undergo a full inorganic geochemical analysis. As such it provides us with the first in-depth opportunity for the development of new inorganic geochemical climate change proxies in peatlands.

2. Relevant previous work on REE and peats

Peats are essentially water logged, humic rich soils that can experience significant water movements, particularly in the upper zone of active plant decomposition. Depending on the trophic status of the peatland, the pH can vary from acidic in ombrotrophic peats (atmospherically fed) to near neutral in minerotrophic peats (receiving surface and ground water inputs as well). Previous research on soils, sediments and aquatic systems found that low pH (Elderfield et al., 1990; Sholkovitz, 1992; Land et al., 1999; Compton et al., 2003) and the presence of organic matter (Aubert et al., 2002; Hodson, 2002; Johannesson et al., 2004) can significantly increase REE solubility. This is in part dependent on the dissolution of certain primary REE minerals (e.g., apatite or feldspar) through reactions with complexing ions present in soil and surface waters. REE can be fixed in soils by (i) retention in weathering resistant primary minerals; (ii) incorporation into newly formed crystalline or amorphous phases; and (iii) by absorption to clays (Minařík et al., 1998).

Several studies demonstrated that during REE mobilisation in crustal weathering the relative REE patterns are not significantly affected (McLennan, 1989). Soil weathering however, does produce fractionation of REE patterns (Land et al., 1999; Aubert et al., 2002; Hodson, 2002; Compton et al., 2003) with heavy REE (HREE: Tb-Lu) preferentially released as they form stronger complexes with ligands in solution than light REE (LREE: La-Nd) (Nesbitt, 1979; Aubert et al., 2002; Compton et al., 2003). In soils this leads to LREE enrichments in more acidic horizons and/or an increase in HREE with depth associated with the more basic conditions of the soil (Minařík et al., 1998; Land et al., 1999; Aubert et al., 2002; Compton et al., 2003). Middle REE (MREE: Sm-Gd) have also been shown to dissolve preferentially when phosphate rich minerals (e.g., apatite) are present (Weber et al., 1998; Hannigan and Sholkovitz, 2001; Ji et al., 2004).

Laboratory trials examining REE leaching from rocks showed that at pH 6 REE/Ca ratios are three times lower than those measured at pH 3. Thus at near neutral pH only

small fractions of REE are leached (Möller, 2002). Experimental systems differ considerably from natural conditions however, where mineral dissolutions occur at reduced rates due to the presence of coatings and the near equilibrium conditions (Möller et al., 1998; Ganor et al., 2005). Feldspars are quite resistant to mild acid leaching in both experimental and natural settings (Möller et al., 1997; Bau et al., 1998) and in peats quartz and felspars are preserved for thousands of years even in acid (pH 4–4.5), organic rich environments (Steinmann and Shotyk, 1997; Le Roux et al., 2006).

Ylirukanen and Lehto (1995) observed REE concentrations in peats varied in conjunction with ash content and that the REE patterns were similar to those of the rocks surrounding the peatland. Past studies showed similar trends between REE (La, Ce, Nd, Sm, Yb and Lu) and other conservative lithogenic elements (Shotyk et al., 2001) and little difference was observed between individual REE profiles with the exception of Eu and Ce (Krachler et al., 2003). Akagi et al. (2002) ascertained that REE concentrations were not significantly influenced during vegetation burial. Aubert et al. (2006) established the immobility of REE in peat and, by comparing REE patterns in peats to snow and lichen samples, that atmospheric REE signals are preserved after deposition.

3. Methodology

3.1. Site description and geological setting and deposit trophic status

Lynch's Crater (S17°22′, E145°42′) in the Atherton Tablelands, NE Queensland, Australia (Fig. 1) experiences a present day annual temperature of 20.4 °C and annual precipitation of 2570 mm. The crater is volcanic in origin and has accumulated lake sediments and peat up to the spill level of the breached southern crater wall. The depth of the deposit is estimated at 60–70 m.

Local rock consists of clinopyroxene, plagioclase and olivine basalts forming the northern part of the Atherton Basaltic Province. This province is Tertiary to Quaternary in age (Stephenson et al., 1980) and volcanic rocks in this region erupted over a variety of basement rocks of Devonian to Early Permian in age, including metamorphosed sediments and granitic rocks (Hodgkinson formation). Up to 22 possible phases of volcanism have been identified that resulted in a complex series of multi-layered basalt units, interspersed with highly weathered soil profiles (Pearce, 2002). The Atherton Basaltic Province is part of the broad zone of intra-plate volcanism that spans some 3000 km along eastern Australia (Ewart et al., 1988).

3.2. Sample collection and preparation

A 13 m long core was collected from the central part of Lynch's Crater in May 2004. A monolith was cut from a hummock to a depth of 10 cm using a stainless steel knife. This was cut into 2 cm increments and packed into plastic bags. A D-section Russian sampler was used to obtain the individual core lengths, which were wrapped in aluminium foil immediately after retrieval. pH was determined by placing a piece of fresh material into Millipore water in a Horiba twin pH meter. In the laboratory, sub-samples were taken at 10 cm increments, placed in plastic bags and freeze-dried. Once dried, samples for geochemistry were milled by hand using a mortar and pestle, sieved with a 500 μm sieve, milled again and then put through a 250 μm sieve. Samples were examined by microscope to remove rootlets. All utensils were thoroughly cleaned between samples using ethanol. Two crater wall soil cores, a basal sediment sample from 62.75 m of depth and rocks from the crater and surrounding area (<10 km radius) were collected during a drilling campaign in November 2004. Soil and sediment samples were dried and ground to <2 μm and rocks were cut and fresh material ground to <20 μm sized particles.

3.3. Deposit characterization

Age dating was performed using the analytical procedures outlined in Fink et al. (2004) and the age/depth model is given in Fig. 2A. The trophic status of the peatland was established based on ash content, pH and Sr concentrations. The top portion of the deposit to a depth of ~150 cm is ombrotrophic characterised by pH values <4.8 and ash contents <5% (Fig. 2B and C) (Tolonen, 1984). Between 150 and 350 cm a transition towards more minerotrophic conditions occurs. From ~350 cm to the base of the profile the pH values vary between 6.0 and 7.6 and ash contents increase >5% (Fig. 2B and C) indicative of fully minerotrophic peat (Muller, 2006; manuscript in preparation).

In the ombrotrophic section all deposited REE are atmospherically derived (denoted as A5 on Fig. 2B). Moderate ash contents (<8% with the exception of A2) and constant REE concentrations in most minerotrophic sections (A1, A3 and A4) suggests that REE are predominantly atmospheric in origin and that there was relatively constant peat accumulation and/or rate of dust addition over time. Increases in ash content as in section A2 (Fig. 2B) could be a result of enhanced decomposition of organic matter/decreased peat accumulation associated with drier environments or increases in non-atmospheric additions.

There are four periods where the ash content of the peat is remarkably high (18–53%): 690–750 cm (P1); 550–600 cm (P2); 480–510 cm (P3) and 150–270 cm (P4). Examination of these layers by SEM found abundant sponge spicules and diatoms suggestive of high algal and protista productivity. These are interpreted as wet periods at Lynch's Crater (Muller, 2006) and are described in a short core taken in July 2003 (Muller et al., 2006). During wet periods (P1–P4) the increased ash content suggests sediment influx and greater surface water movements, which would overprint atmospheric REE signals.

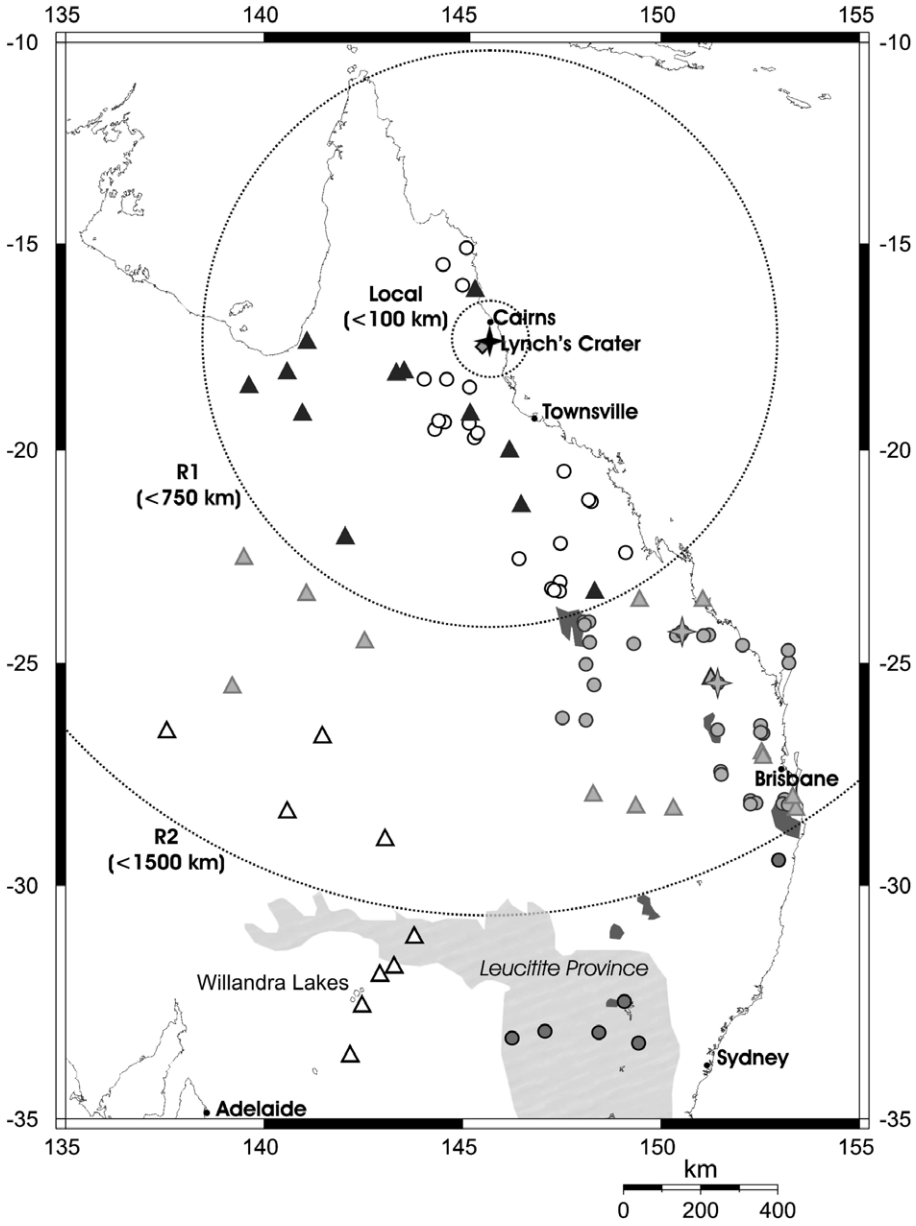

Fig. 1. Map showing the location of Lynch's Crater in NE Queensland, Australia and the location of samples used in source tracing of deposited dusts. Circles represent Cenozoic lava samples (Ewart et al., 1988; Zhang et al., 2001) while triangles represent alluvial and surface sediment samples (Kamber et al., 2005; Marx et al., 2005a,b). The source region boundaries (Local, R1, R2 and LD) were defined using transport distances of different aerosol size fractions (Warneck, 2000). Dark grey shaded areas represent central volcanic provinces while the large light grey shaded area represents the leucitite volcanic province in New South Wales and Victoria.

3.4. Materials and reagents

All solutions were prepared using purified water from an 18 MΩ cm grade Millipore system (Bedford, USA). Acids were analytical grade Aristar (Merck, Darmstadt, Germany) except for those used in ion exchange column chemistry and Pb isotope measurements, which were ultra-pure grade from Romil (Cambridge, UK). All work was performed under clean laboratory conditions (laminar flow hoods, HEPA-filtered air, protective clothing and footwear) and all labware was cleaned in heated acid baths (10% HCl or 10% HNO_3) prior to use.

3.5. Chemical and physical properties

The percent inorganic content was determined by dry ashing peat samples overnight at 450 °C, expressing results as a percentage of the dry weight of the sample at 105 °C.

Peat samples were prepared for elemental analysis by placing 0.500 g of material into a PTFE test tube, adding 8.0 ml HNO_3 and leaving the sample heated to 50 °C overnight. Tubes were then removed and 5.0 ml HF and 1.0–2.0 ml $HClO_4$ added. This was then heated for 3 h at 90 °C, 3 h at 140 °C and left overnight at 170–190 °C. To the resultant dry residue 2.0 ml 5 M HCl was added and

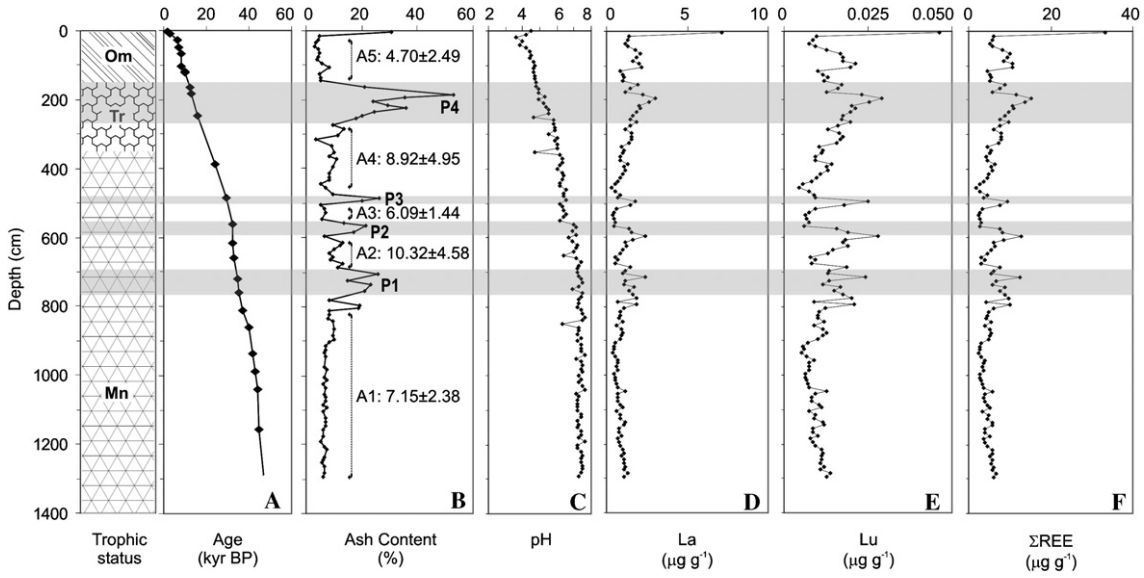

Fig. 2. Examination of the trophic status finds the deposit is comprised of minerotrophic peat (Mn) which transitions (Tr) to ombrotrophic peat (Om) in upper layers. The age model (A) dates the record at 52 kyr while the ash profile reveals periods of atmospherically dominated inputs (A1–A5) as well as the existence of four wet events (P1–P4) (B). Also shown are the profile pH variations (C) and La (D), Lu (E) and ΣREE (F) concentrations with depth.

samples were leached for an hour at 60 °C. The sample, remaining solution and 8.0 ml H_2O was then mixed using a vortex mixer and decanted into new test tubes. Solutions were diluted with 2% HNO_3 for analysis by ICP-MS and ICP-OES.

Soil and rock samples were weighed to 0.100 g, placed into PTFE test tubes and digested using an initial acid mixture of 2.0 ml HNO_3, 1.0 ml $HClO_4$ and 5.0 ml HF. Samples then underwent the same heating program as described above. To the resultant residue 2.0 ml of 4 M HCl was added which was then heated for an hour at 70 °C. The sample, remaining solution and 8 ml H_2O were mixed using a vortex mixer and decanted into new test tubes. Solutions were diluted with 2% HNO_3 for analysis by ICP-MS and ICP-OES.

Elemental concentrations were determined using a Varian ICP-MS. Detection limits were 0.6 pg g^{-1} in solution or better for REE (La, Ce, Pr, Nd, Sm, Eu, Gd, Tb, Dy, Ho, Er, Tm, Yb and Lu) and 3 pg g^{-1} in solution or better for selected elements (As, Cu, Pb, Sc, Sr, Y and Zr). Blank levels for REE were <2.8%. Average elemental blanks were <15% for Sc and Pb and <5.1% for all other analysed elements. Additional elements (Al, Ca, Fe, Mg, Na, P, S, Ti and V) were determined using a Varian Vista Pro ICP-OES. Detection limits in solution were <0.01 μg g^{-1} and <0.05 μg g^{-1} for trace and major elements, respectively. Blank levels were <3.1% for all elements.

3.6. Pb isotope analysis

Peat samples were measured for Pb isotopes during sessions in August 2004 and January 2005. Peat core samples were prepared for isotope analysis using a previously developed peat sample preparation procedure (Kylander et al., 2004). This procedure involved dry ashing bulk peat samples followed by digestion using a Microwave Accelerated Reaction System (MARS)-X (CEM, Mattheus, USA). The acid mixture varied the amount of HF depending on the ash weight, using a ratio of 0.16 ml HF: 50 mg ash. After digestion, samples were evaporated to dryness and Pb isolated by ion exchange column chemistry using a selective extraction chromatographic resin from EiChrom as described elsewhere (Weiss et al., 2004).

Isotopic measurements were made on an *Isoprobe* MC-ICP-MS (GVi, Manchester, UK) at the Natural History Museum London. This instrument is equipped with a CETAC desolvator and a T1H concentric nebuliser for sample introduction. Static collection for Pb analysis used the seven independently adjustable Faraday cups set at the following masses: 200 (Hg), 203 (Tl), 204 (Pb), 205 (Tl), 206 (Pb), 207 (Pb) and 208 (Pb). NIST-SRM 981 Pb standards and sample solutions were spiked with NIST-SRM 977 Tl. Samples and standards were adjusted to a consistent Pb/Tl ratio of 2:1. Averaged acid blank intensities were subtracted from raw sample isotopic intensities to correct for Faraday cup offset and instrumental and solvent blanks. Corrections for Hg interference on ^{204}Pb, as monitored by ^{200}Hg, were typically ⩽0.1%. Instrumental mass bias was corrected by using isotope ratios from the spiked NIST-SRM 981 standard measurements in a least squares optimisation as described in Weiss et al. (2004). Procedural blanks were <1% of the total Pb based on intensity data.

4. Results

4.1. Analytical performance

No certified peat reference material exists so soil and plant reference materials were used to quantify analytical accuracy. Using a combination of HF–HNO_3–$HClO_4$ in

externally heated open vessels, REE recoveries using the soil reference material GBW Chinese Soil 07406 (Institute of Geophysical and Geochemical Exploration, Langfang, China) were 55–94%. There was no systematic change in recovery across the REE. In-house plant reference materials Grasses HRM 12 and 14 showed La recoveries between 51% and 82%. These results are typical of open vessel digests and likely reflect the incomplete dissolution of minerals like zircon (Yang et al., 2002). As all samples were prepared using the same method however, relative differences are real. REE concentrations determined in sampled local rocks are in the same range given by Zhang et al. (2001) for Atherton basalts (Fig. 3A and B). This work reports an analytical accuracy of 5% against their in-house standard Kilauea 93–1489 providing significant confidence to our results. Trace and major element recoveries for soil and plant reference materials were higher, generally within 10% of the certified values. Sample duplicates were prepared to check precision and average deviations of 9.5% (2σ) (range: 0–32%) were found.

The long-term reproducibility of Pb isotope measurements ($^{206}Pb/^{204}Pb$, $^{207}Pb/^{204}Pb$, $^{208}Pb/^{204}Pb$, $^{207}Pb/^{206}Pb$ and $^{208}Pb/^{206}Pb$) based on repeat measurements ($n = 381$) of NIST-SRM 981 Pb acquired during sessions from June 2003 to September 2005 was used as an estimate of precision; most Pb isotope ratio changes measured are significantly different at the 95% confidence level (2σ). Precisions on individual Pb isotope ratios expressed relative to the mean (in ppm) were: 209 for $^{206}Pb/^{204}Pb$, 296 for $^{207}Pb/^{204}Pb$, 350 for $^{208}Pb/^{204}Pb$, 321 for $^{206}Pb/^{207}Pb$ and 352 for $^{208}Pb/^{206}Pb$. Accuracy was determined based on repeat measurements of NIST-SRM 981 Pb ($n = 381$) evaluated against values published by Galer and Abouchami (1998). Accuracies for individual Pb isotopes expressed relative to the mean (in ppm) were: 6 for $^{206}Pb/^{204}Pb$, 168 for $^{207}Pb/^{204}Pb$, 519 for $^{208}Pb/^{204}Pb$, 159 for $^{206}Pb/^{207}Pb$ and 511 for $^{208}Pb/^{206}Pb$. In attempts to characterise reproducibility in a heterogeneous sample matrix like peat, an in-house peat reference material (CND 1) was also prepared and measured each session. The precision using this material expressed relative to the mean (in ppm) was: 496 for $^{206}Pb/^{204}Pb$, 359 for $^{207}Pb/^{204}Pb$, 772 for $^{208}Pb/^{204}Pb$, 613 for $^{206}Pb/^{207}Pb$ and 957 for $^{208}Pb/^{206}Pb$ ($n = 13$, 2σ); this is approximately two times greater than that estimated using a synthetic solution like NIST-SRM 981 Pb.

4.2. REE concentrations in peat profiles

Overall concentration ranges for each REE (in $\mu g\ g^{-1}$) were: La 0.33–7.16; Ce 0.66–11.94; Pr 0.09–1.69; Nd 0.36–6.91; Sm 0.073–1.43; Eu 0.02–0.44; Gd 0.077–1.42; Tb 0.011–0.20; Dy 0.057–1.02; Ho 0.011–0.18; Er 0.030–0.46; Tm 0.0042–0.057; Yb 0.029–0.34 and Lu 0.0044–0.046. Total REE ranged between 1.75 and 33.29 $\mu g\ g^{-1}$. Full REE concentration data for all peat samples is provided in Electronic Annex 1. Fig. 2D–F shows the concentration profiles for La, Lu and ΣREE. Individual REE profiles show little variation at the base (805–1295 cm). Elemental concentrations increase during wet periods (P1–P4 on Fig. 2B) but decrease again when peat accumulation resumes (A1–A5 on Fig. 2B).

4.3. REE patterns, Eu and Ce anomalies of source rocks and peats

Post-Archean Australian shale (PAAS; Taylor and McLennan, 1985) normalised REE patterns of rocks sampled locally (<10 km from the crater) are compared to those of basalts from the Atherton Province (Zhang et al., 2001) in Fig. 3A and B. To accomplish source tracing of deposited dusts local rocks were divided into Groups I and II based primarily on Eu anomaly, but REE patterns were considered as well. Group I includes material from a surface volcanic ash outcrop (A), crater wall soil samples from 280 to 385 cm of depth (CW280 and CW385) and a crater rim rock sample (R3). Group I $(Eu/Eu^*)_{PAAS}$ range between 1.19 and 1.38. LREE fractionation relative to HREE (expressed by $(La/Lu)_{PAAS}$) ranges between 0.94 and 1.79 while MREE fractionation relative to HREE (expressed by $(Gd/La)_{PAAS}$) falls between 1.38 and 2.87. Group II is comprised of rock samples (R1, R2 and R4) from the crater rim and a shallow crater wall soil sample (CW180). $(Eu/Eu^*)_{PAAS}$ values range from 0.96 to 1.09, which is lower than that of samples from Group I. The $(La/Lu)_{PAAS}$ and $(Gd/La)_{PAAS}$ ranges for this group are 1.46–1.75 and 2.01–2.39, respectively. Full REE concentration data for local rocks is provided in Electronic Annex 1.

REE patterns from peat core samples (as represented by a sample from each metre of the core) normalised to PAAS show relatively flat patterns with positive Eu anomalies (Fig. 3C). REE concentrations in the peats are an order of magnitude lower than PAAS. Peat samples were also normalised using the average REE concentrations at the base of the profile (1195–1295 cm) where REE values and ash contents are relatively constant. Fig. 4 shows that the most striking change in patterns is in terms of Eu anomaly. This is better recognized on the plot of $(Eu/Eu^*)_{PAAS}$ with depth given in Fig. 5A showing peat sample values ranging between 1.09 and 1.48. From the base of the profile to a depth of 825 cm values vary around a mean of 1.40 ± 0.09 ($n = 48$, 2σ). The decrease that starts at 825 cm stabilizes at an average value of 1.18 ± 0.05 ($n = 46$, 2σ) between 145 and 595 cm. In the upper metre of the core the values increase to an average value of 1.37 ± 0.06 ($n = 11$, 2σ).

In addition to differences in $(Eu/Eu^*)_{PAAS}$, some samples in Fig. 4 show greater fractionation. $(La/Lu)_{Profile}$ and $(Gd/Lu)_{Profile}$ vs. depth changes shown in Fig. 6A and B reveal that the majority of peat samples are within 1σ of the mean. LREE depletions occur between 615 and 675 cm (A2) and 465 and 565 cm (A3) and enrichments occur between 5 and 75 cm (upper A5). Slight MREE depletions occur at 615–685 cm (P2), 535 cm, 515 cm and 385 cm while enrichments occur at 575 cm and 5–75 cm.

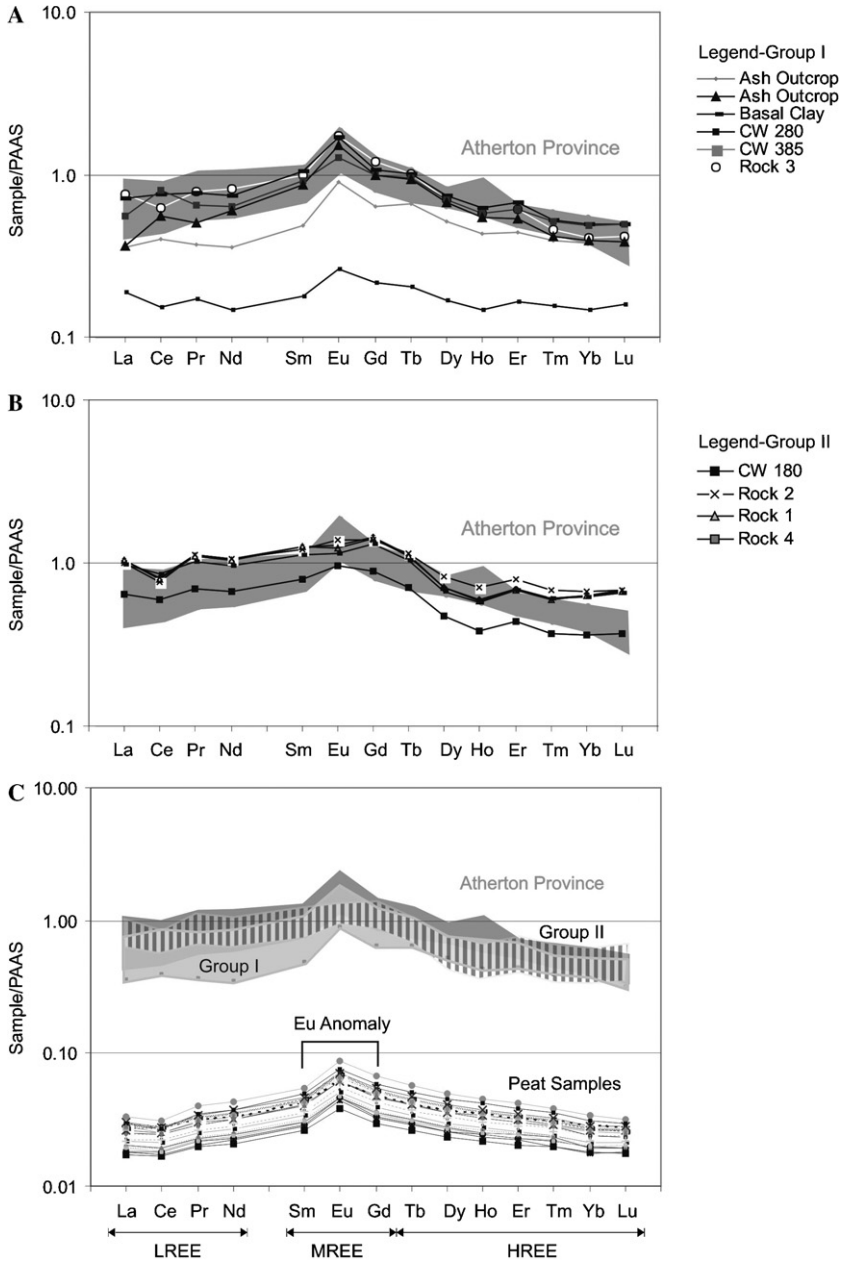

Fig. 3. PAAS normalised REE patterns from Group I (A) and Group II (B) local source rocks compared to those from Atherton basalts (shaded area) (Zhang et al., 2001) confirms that Group I is representative of the dominant local lithology. PAAS normalised peat samples (one sample per metre) match Group I (light grey) and Atherton basalt (dark grey) patterns rather than those of Group II (hatched) source rocks (C).

The $(Ce/Ce^*)_{PAAS}$ profile is given in Fig. 5B. The majority of samples are within 1σ of the mean of 0.91 ± 0.03. While some samples, namely those between 1265 and 1295 cm, have more negative anomalies the largest changes occur between 35 cm and the surface where $(Ce/Ce^*)_{PAAS}$ reaches the most negative value of the profile (0.79).

4.4. Pb concentrations and isotopes

Lead concentrations vary between 0.26 and 4.10 μg g^{-1} (average: 0.78 ± 0.87 μg g^{-1}, $n = 130$, 2σ) (Fig. 7A) while Pb/Sc values range between 0.24 and 2.71 (average: 1.29 ± 0.75, $n = 130$, 2σ) (Fig. 7B). $^{206}Pb/^{207}Pb$ isotope ratios have a range of 1.1474–1.2176 (average: 1.2017 ± 0.0234, $n = 95$, 2σ) (Fig. 7C). The base of the profile (782.5–1293.5 cm) varies erratically from 1.1750 to 1.2149 while the remainder (5–755 cm) shows less spread, ranging between 1.1951 and 1.2176 with the exception of peaks at 443 cm (1.1838), 105 cm (1.1697) and 5 cm (1.1474). Group I source rocks are less radiogenic ($^{206}Pb/^{207}Pb = 1.19$–1.23) than Group II source rocks ($^{206}Pb/^{207}Pb = 1.24$–1.29). Full Pb isotope data for peat and rock samples is provided in Electronic Annex 2.

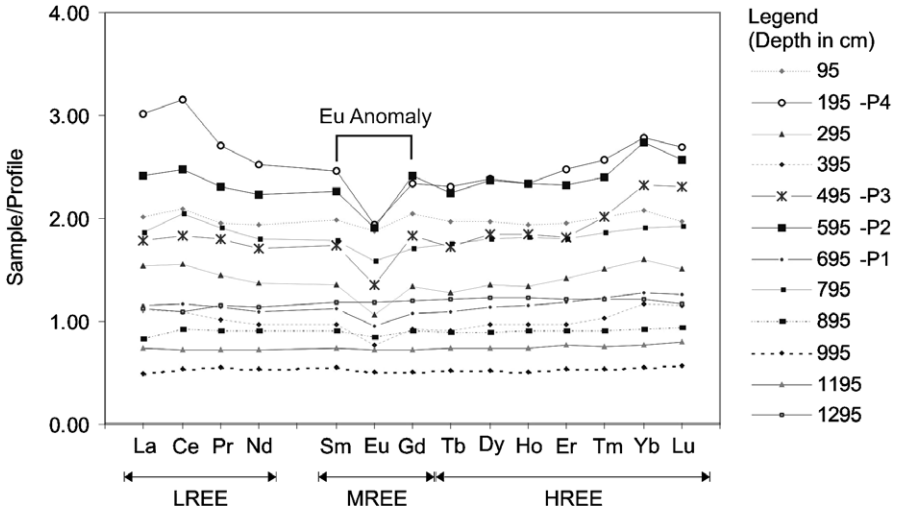

Fig. 4. REE patterns of peat samples, as represented by a single sample from each metre, normalised to the base of the profile (915–1295 cm) show there is no clear pattern of changing REE concentrations with depth. Several samples do show greater degrees of LREE, MREE and HREE fractionation.

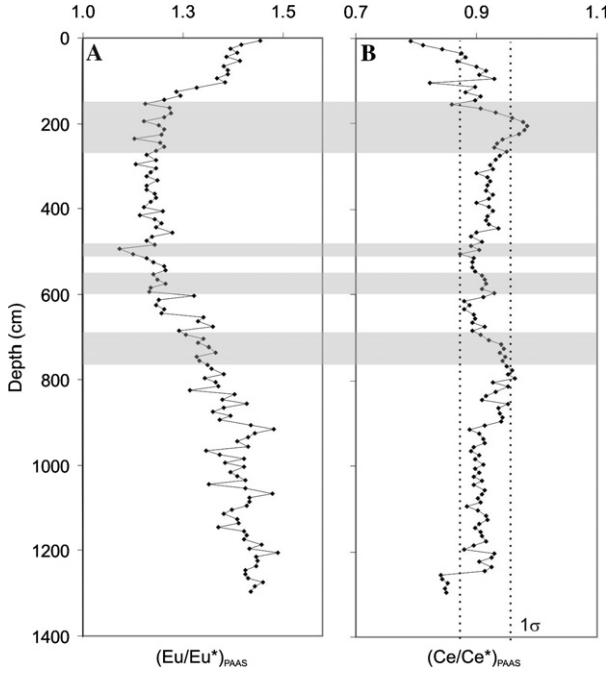

Fig. 5. $(Eu/Eu^*)_{PAAS}$ and $(Ce/Ce^*)_{PAAS}$ vs. depth. Given for Ce is range of $\pm 1\sigma$ from the mean. Shaded zones represent wet events.

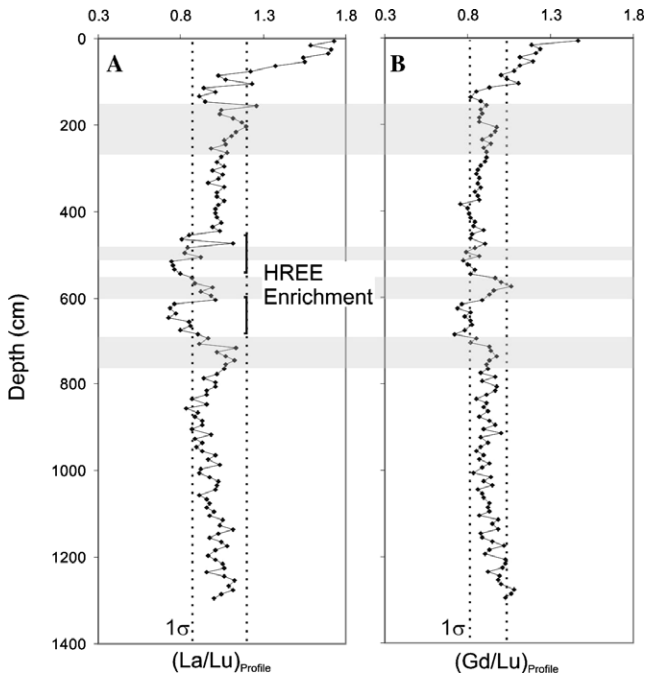

Fig. 6. LREE (A) and MREE (B) fractionation relative to HREE as calculated by $(La/Lu)_{PAAS}$ and $(Gd/Lu)_{PAAS}$, respectively. Dashed lines are $\pm 1\sigma$ from the mean. Shaded zones represent wet events.

5. Discussion

5.1. Representativeness of the peat core

Bindler et al. (2004) suggested significant with-in bog variations in elemental concentrations (but not lead isotopes) occur and recommend multi-core studies for accurate reconstruction of atmospheric deposition at a site. In addition to the long core discussed here, Ca, Al, Mg and ash content were determined in a short core (6 m) taken from Lynch's Crater in July 2003 (Muller et al., 2006). Comparison of these two cores shows similar trends in elemental concentrations and ash contents. This agreement is likely due to (i) the age of the material such that compaction smoothes out micro-scale variations; and (ii) the deposit is relatively small (600 m^2) and resting in a crater thus it has not been subject to the same stress-strain dynamics of open deposits, resulting in less significant hummock and hollow formation (a hypothesized factor in generating the observed with-in bog variations).

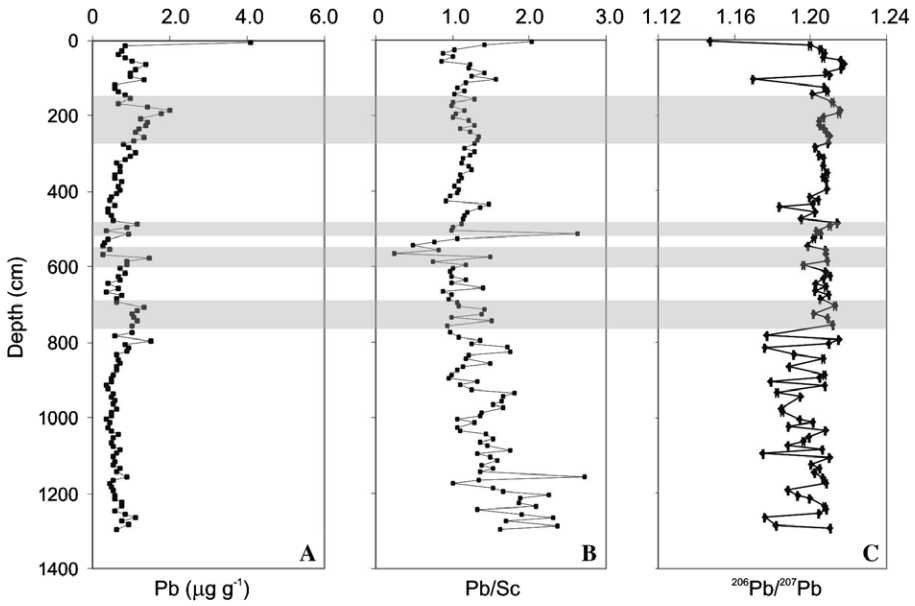

Fig. 7. Pb concentrations (A), Pb normalised to Sc (B) and $^{206}Pb/^{207}Pb$ (C) variations with depth. Pb isotope error bars are estimated from repeat measurements of NIST-SRM 981 Pb. Shaded zones represent wet events.

5.2. Internal processes: characteristics of REE within the deposit

5.2.1. Immobility of REE

Correlation coefficients indicate individual REE vary in the same manner within the deposit with r values >0.93 ($n = 130$, $\alpha = 0.05$). Europium is the sole exception having slightly lower correlations with Yb ($r = 0.88$) and Lu ($r = 0.90$); this is not unexpected as the behaviour of Eu is distinct from other REE during high temperature processes. The high correlation between individual REE, especially Ce, which is redox sensitive at low temperatures (McLennan, 1989), suggests these elements are immobile.

To account for variations in peat accumulation, REE were normalised to Al and Ti. Normalised La, Lu and ΣREE profiles are shown in Fig. 8A–F with upper continental crust (UCC) values given for reference (Wedepohl, 1995). Peaks occur at 715, 595 and 505 cm on Al and Ti normalised plots with the latter also showing a peak at 1205 cm. The reason for this is unclear but Ti concentrations at this depth are noticeably low. Importantly, there are no high REE concentration horizons (other than during wet periods) or increasing REE with depth as seen in weathered soil profiles (Minařík et al., 1998; Land et al., 1999; Aubert et al., 2002; Compton et al., 2003). Although pH is a dynamic property of the deposit, affected by mire hydrology and climatic conditions, the current pH values correlate weakly ($r < 0.4$) with REE concentrations. REE patterns vary little the length of the profile and do not show any concentration vs. depth relationship (Fig. 4).

A principal component analysis (PCA) was performed on all elemental data (Al, Ca, Cu, Fe, Mg, Na, P, Pb, REE, S, Sc, Sr, Ti, V, Y and Zr) using Minitab statistical software. A correlation matrix was employed to weight each variable equally. The topmost sample (5 cm) was excluded from this analysis due to its anomalously high REE concentrations, possibly a result of anthropogenic activities such as petroleum refining (Krachler et al., 2003) and/or surface compaction by cattle grazing, burning of vegetation, drainage, peat extraction, etc. The first component, explaining 52.5% of variance in the data consists of the entire REE suite and elements known to be immobile in peats, namely Al, Pb, Sc, Ti, Y and Zr (PC1, Fig. 9). The second component (PC2, Fig. 9), explaining 16.9% of the variance, grouped together established mobile elements including Ca, Fe, Mg, Na and Sr.

Elemental correlations can infer (although not confirm) possible mineralogical relationships (Condie, 1991; Roy and Smykatz-Kloss, in press). Individual and total REE and P in peat samples show no correlation suggesting that minerals like apatite ($Ca_5[PO_4]_3[OH, F, Cl]$) and monazite ($[Ce, La, Th, Nd, Y]PO_4$) are not primary REE hosts. Many studies suggest that the bulk of REE reside principally in clays bound in the mineral lattice and absorbed onto their surfaces (Gallet et al., 1996; Gallet et al., 1998; Yang et al., 2002; Gaiero et al., 2004). The moderate correlation between REE and Al ($r = 0.5$–0.7) indicates clays may be important hosts at Lynch's Crater. Moderate to high correlations ($r = 0.8$–0.9) between REE and Zr indicate zircon could also play a role in hosting deposited REE, particularly HREE (Condie, 1991).

The evidence presented above confirms REE immobility within the peat deposit which is in agreement with the recent work of Aubert et al. (2006).

5.2.2. Post depositional environment

Little is known about pore water–mineral interactions in the organic rich, anoxic, varying pH conditions occuring in

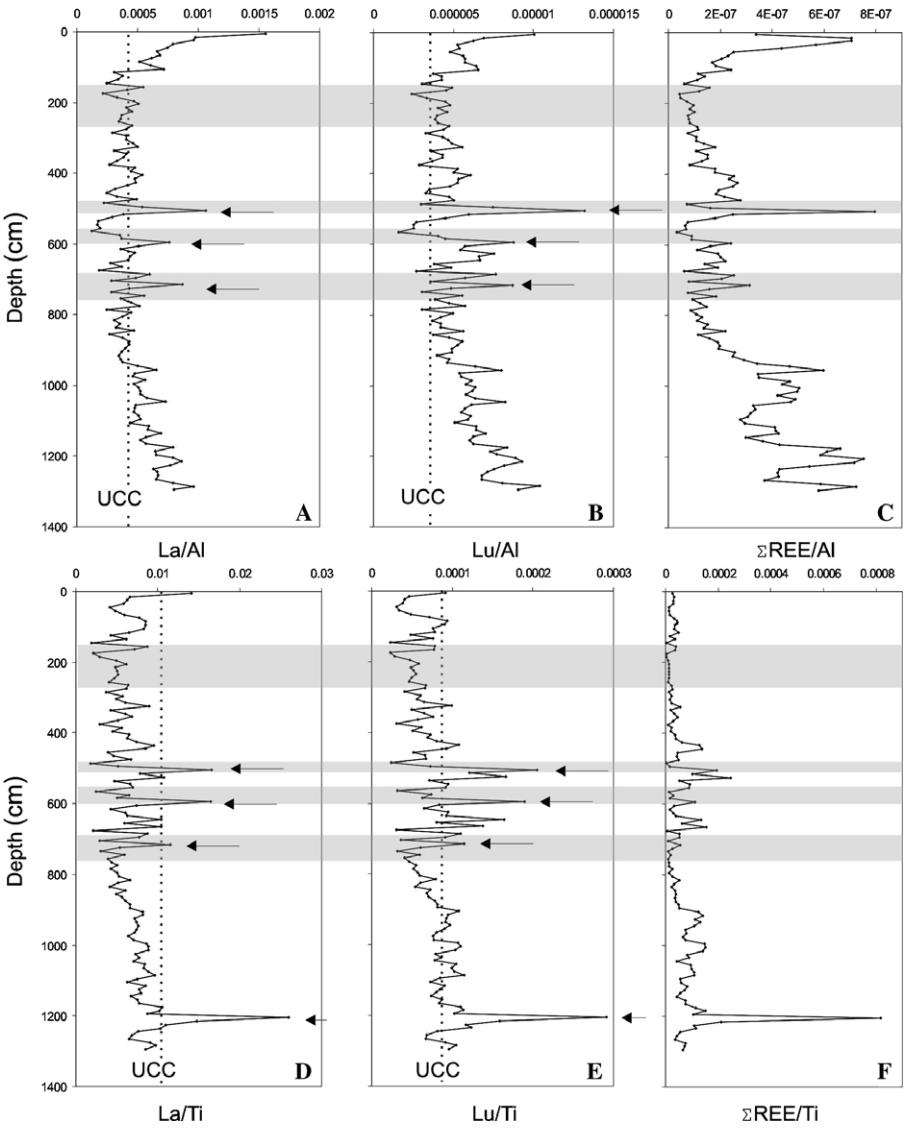

Fig. 8. La, Lu and ΣREE profiles normalised to Al (A–C) and Ti (D–F). One peak on Ti normalised plots is not evident on Al normalised plots. Generally, peaks occur during the wet events shown in shaded areas. The dashed lines give the UCC values (Wedepohl, 1995).

mires. During rock–water interactions the formation of secondary phases and the transport capacity of the fluid have been cited as important factors/processes in REE mobility (Bau et al., 1998). The dusts deposited at Lynch's Crater have likely undergone some degree of weathering prior to deposition. Work on tholeiitic basalts from SE Australia found that REE released during weathering were retained either in secondary clay or phosphate minerals; the latter are known to be resistant to leaching (Price et al., 1991). Given the uniformity of peat sample REE patterns (Fig. 4), and their coherence to local rock REE patterns (Fig. 3), it appears advanced weathering has not occurred in contributing dust source areas, which would have fractioned REE more significantly as seen in e.g., laterites (Braun et al., 1993).

The available data does not allow us to predict if any REE are lost through leaching but reasonable constraints can be made. Leaching studies show that at near neutral pH, as in the minerotrophic sections (6–7.6) of Lynch's Crater, only small fractions of REE are lost (Möller, 2002). Both quartz and feldspar are conserved even at low pH (3.5–4.5) possibly through the formation of protective organic matter or mineral coatings. Thereby, even REE in the more acidic (3.6–4.9) ombrotrophic portions are retained (Möller et al., 1997; Steinmann and Shotyk, 1997; Bau et al., 1998; Ganor et al., 2005; Le Roux et al., 2006). While the ground water dynamics at Lynch's Crater are unknown, currently observed surface water movements suggest this is not a highly flushed system, which would also minimise REE leaching and loss.

In general, the peat profile shows Ce anomalies that vary closely around the mean (0.91 ± 0.03) (Fig. 5B) indicating that the development of these anomalies may be chemically or physically inhibited. If Ce and REE in pore waters exist as organic complexes, precipitation of Ce may be prevented or even masked (Dia et al., 2000). Akagi et al. (2002) found

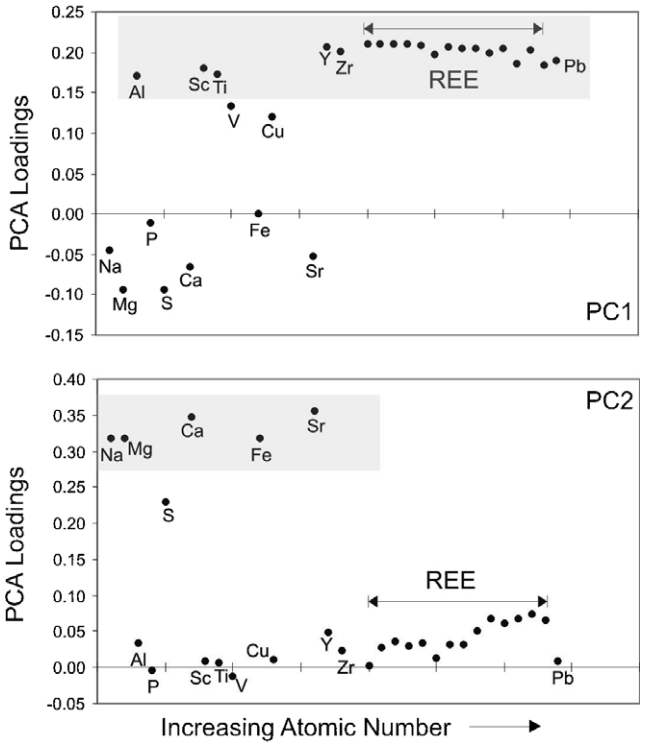

Fig. 9. Plots of principal components one (PC1) and two (PC2). PC1 explains 52.5% of the variance in the data and groups REE with elements know to be immobile in peats (shaded area). PC2 explains 16.9% of the variance and is composed of elements known to be mobile in peat (shaded area).

little evidence of Ce anomalies in mire vegetation samples from the Ozegahara peatland in Japan and suggest the prevailing E_H and pH (<8) conditions in mires are not favourable to Ce anomaly development. Negative anomalies are however generated at low pH (~4) and higher E_H (>0.2), which may explain the negative anomalies seen in the top 35 cm of the core.

5.3. External processes: tracing deposited dusts using REE

5.3.1. REE patterns and fractionation

The REE composition of dusts is controlled by source rock, weathering mechanisms and atmospheric transport dynamics between sources and the depositional environment e.g., grain size sorting (Compton et al., 2003; Yang et al., 2004). The absence of REE pattern differentiation demonstrated in profile normalised peat REE patterns (Fig. 4) precludes using these alone for accurate tracing of deposited dusts. The REE patterns of peats, Group I and Atherton Province Basalts (Fig. 3C) show a comparable MREE enrichment relative to PAAS, representative of the dominantly volcanic lithology in eastern Australia (Kamber et al., 2005). Variations in LREE, MREE and HREE fractionation are too small to be informative in terms of source tracing (Fig. 6A and B). This homogeneity suggests that dust source areas are not sufficiently chemically distinct at this location to generate unique REE patterns and/or there is efficient mixing of dusts during transport.

5.3.2. Eu anomalies

Gallet et al. (1998) note that loess regions worldwide have characteristic Eu anomalies stemming from their different provenance areas. Eu anomalies are associated with rock formation (Taylor and McLennan, 1985; Bau, 1991; Wilson, 2000) and the observed changes in $(Eu/Eu^*)_{PAAS}$ must be inherited differences from contributing dust sources. Group I and Group II have $(Eu/Eu^*)_{PAAS}$ ranging between 1.19–1.38 and 0.96–1.09, respectively. Atherton basalts, as measured by Zhang et al. (2001), agree with Group I REE patterns, concentrations and Eu anomalies (1.29–1.43) (Fig. 3A). The upper Eu anomaly range of these potential local source rocks is below that of the peat samples (1.09–1.48) signifying a non-local source must exist.

In order to identify the location of this high $(Eu/Eu^*)_{PAAS}$ dust source area, REE data from Cenozoic lavas collected from eastern Australia, including the Atherton Basaltic Province (Ewart et al., 1988; Zhang et al., 2001); alluvial sediments from Proterozoic and Cenozoic blocks in Queensland (Kamber et al., 2005); and surface sediments from known Australian dust source areas (e.g., Simpson Desert, Lake Eyre) (Marx et al., 2005a;Marx et al., 2005b) were compared to peat core data (see Table 1 for data sources, Fig. 1 for sample locations). These are plotted

Table 1
The geographical range definitions and samples types used in source tracing of deposited dusts

Source groups	Distance from sampling site	Sample type	Reference
Local			
Group I	<10 km	Local rock (Ash Outcrop, Crater Wall 280 and 385 cm, Rock 3)	This study
Group II		Local rock (Rock 1, 2 and 4, Crater wall 180 cm)	This study
Atherton	<100 km	Cenozoic basalts	Zhang et al. (2001)
Regional			
R1	<750 km	Cenozoic basalts	Zhang et al. (2001)
R2	<1500 km	Cenozoic lavas	Ewart et al. (1988)
		Alluvial sediments	Kamber et al. (2005)
		Surface sediments	Marx et al. (2005a,b)
Long distance			
LD	>1500 km	Cenozoic lavas	Ewart et al. (1988)
		Surface sediments	Marx et al. (2005a,b)

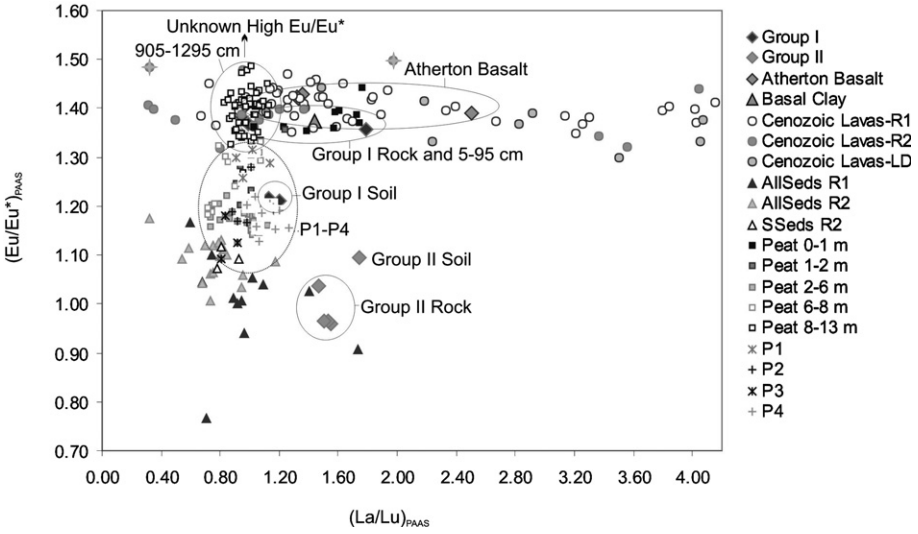

Fig. 10. Plot of $(Eu/Eu^*)_{PAAS}$ vs. $(La/Lu)_{PAAS}$ including peat samples (squares); local sources (diamonds): Group I and II (this study) and Atherton Cenozoic basalts (Zhang et al., 2001); and regional and long-distance sources (triangles for alluvial and surface sediment samples, circles for Cenozoic lavas) (Ewart et al., 1988; Kamber et al., 2005; Marx et al., 2005a,b). Wet events are also indicated.

as $(La/Lu)_{PAAS}$ vs. $(Eu/Eu^*)_{PAAS}$ in Fig. 10 where distinction has been made between local (<100 km), regional (R1 < 750 km, R2 < 1500) and long-distance (LD > 1500 km) sources as defined by grain-size-transport distances (Warneck, 2000).

Crater wall soil samples reveal mixing between Group I/Atherton basalts and Group II type signatures. If only rock samples are considered, a binary mixing equation using Eu anomaly data from Group I/Cenozoic lavas ($(Eu/Eu^*)_{PAAS} = 1.30–1.50$) and Group II ($(Eu/Eu^*)_{PAAS} = 0.96–1.09$) shows that Group II type rocks increase in importance between 105 and 895 cm (8525–40,815 BP) (Fig. 11). In the broad lava plain of the Atherton Basaltic Province, covering some 1800 km^2, Group I/Atherton basalt type rocks are lithologically dominant. The increased importance of Group II type rocks at these depths is unlikely a consequence of their preferential weathering. Rather, given the considerable overlap between Group II and available data from R1 and R2 alluvial and surface sediments, these sources must become dominant at this time.

Peat samples from the basal portion of the profile (905–1295 cm, 41,095–52,505 BP) display the highest in core $(Eu/Eu^*)_{PAAS}$ values (1.30–1.48). It seems the upper $(Eu/Eu^*)_{PAAS}$ range for Group I/Cenozoic lavas is too low; as it is presently defined (1.50) these source groups would contribute at a minimum 42–96% of the dusts deposited at these depths. There are only two source samples, located in R2, that exceed the Eu anomaly range found in the peat samples (indicated as stars on Figs. 1, 10 and 12). The volcanic provinces of eastern Australia are classed as one of three types: leucitite (light grey shaded area Fig. 1), lava-field and central-volcano (dark grey shaded areas Fig. 1). Lava-field provinces like the Atherton Basaltic Province, and indeed all of northern Queensland, have less differentiated lavas (i.e., no plagioclase separation, thus lower Eu anomaly) compared to the other volcanic provinces of eastern Australia (Ewart et al., 1988). Central volcano

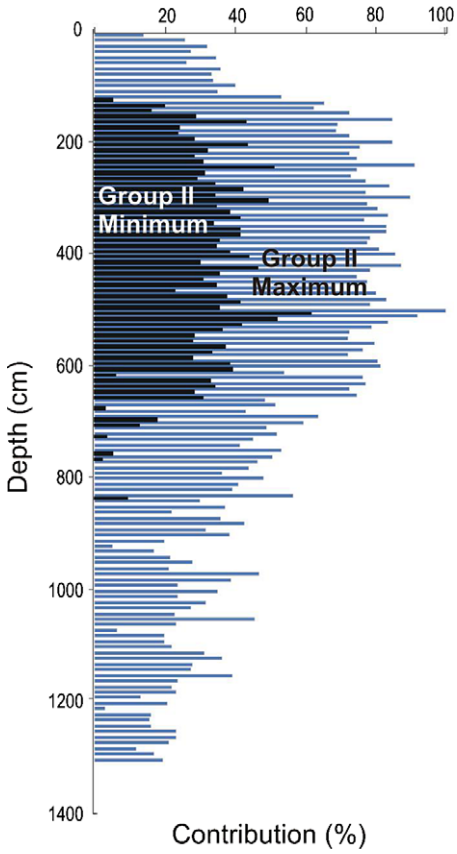

Fig. 11. Maximum and minimum contributions of Group II type sources to the Eu anomalies measured in the peat samples. The lighter shaded area thus represents the possible range of Group II contributions.

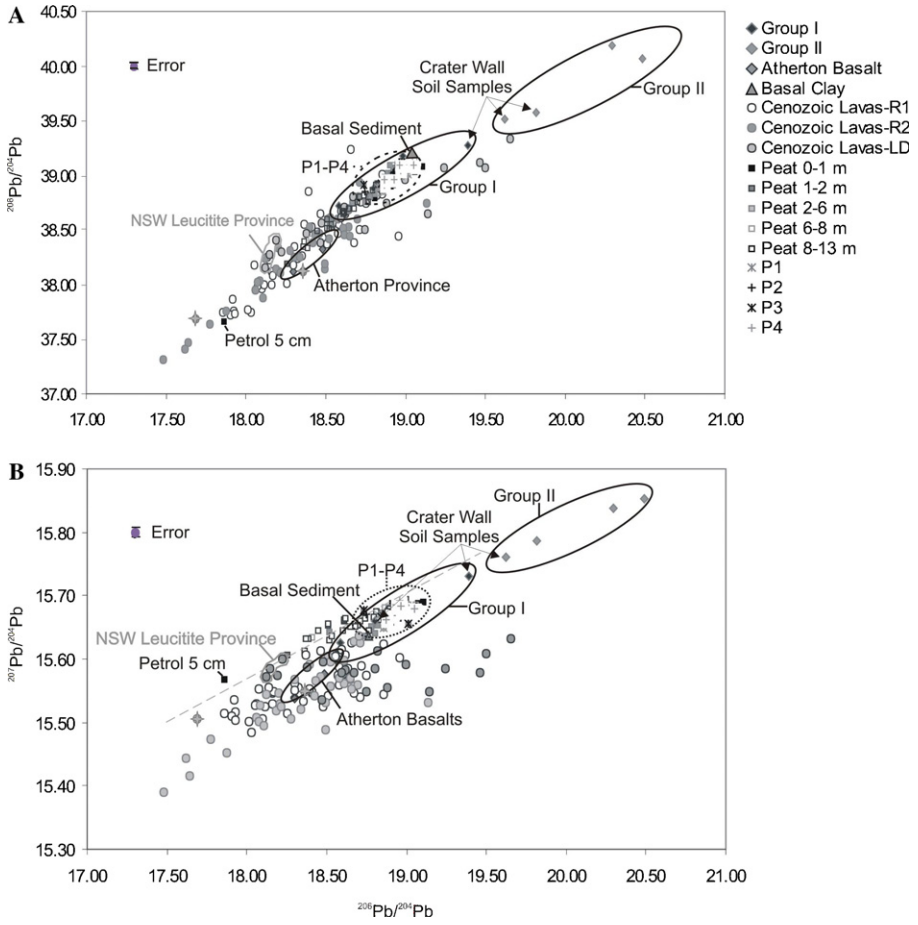

Fig. 12. Three isotope plots of $^{208}Pb/^{204}Pb$ (A) and $^{207}Pb/^{204}Pb$ (B) against $^{206}Pb/^{204}Pb$ showing peat samples (squares); local sources (diamonds): Group I and II (this study) and Atherton Cenozoic basalts (closed diamonds, Zhang et al., 2001); and regional and long-distance lavas (circles) (Ewart et al., 1988). Note there was no Pb isotope data for alluvial and surface sediment samples. Wet events and the basal sediment sample are indicated.

provinces have a high proportion of differentiated rocks such as rhyolites, trachytes and phonolites (Ewart et al., 1988) which could supply the Eu rich dusts that explain the observed basal values. The central volcano provinces in closest proximity to Lynch's Crater are located in R2 in SE Queensland and further to the south in New South Wales (Fig. 1). If central volcano provinces in R2 were as important during this period (41,095–52,505 BP) as they were between 8525 and 40,815 BP, the observed Eu anomaly in the latter should have been greater. Therefore dust sources further to the south (>1500 km) must supply these relatively Eu rich dusts. Long distance sources to the west and south-west (e.g., Simpson Desert, Lake Eyre and Darling River) are excluded based on their Eu anomalies, which range from 0.96 to 1.12. These sources may have been active at other times during the record but due to their similarity with R1 and R2 sources, cannot be clearly quantified.

Examination of the top metre of the core (5–95 cm, 1740–8390 BP) sees all but one sample (5 cm) fall into the source field defined by Group I on the plot of $(La/Lu)_{PAAS}$ vs. $(Eu/Eu^{*})_{PAAS}$ (Fig. 10) implying the majority of the influence is local at this time.

5.3.3. Pb isotopes

Lead isotopes have been applied previously to trace deposited dusts (Rosman et al., 1997; Shotyk et al., 2001; Kylander et al., 2005) and Pb is known to be immobile in peat (Bindler et al., 2004; Shotyk et al., 2005 and references therein). Both Pb and REE are largely incorporated into accessory phases and subject to release under similar weathering conditions (Harlavan and Erel, 2002). By independently reconstructing changes in dust source using Pb isotopes, the validity of the novel $(Eu/Eu^{*})_{PAAS}$ tracing tool can be assessed.

Group I source rocks are less radiogenic ($^{206}Pb/^{207}Pb = 1.19–1.23$) than those from Group II ($^{206}Pb/^{207}Pb = 1.24–1.29$). The Pb isotope signature of Group I is similar to that published by Zhang et al. (2001) for Atherton basalts of 1.17–1.19. As a group the Cenozoic lavas of eastern Australia have $^{206}Pb/^{207}Pb$ values ranging between 1.13 and 1.25 (Ewart et al., 1988). As mentioned before, the surface sample at 5 cm is anthropogenically impacted (Fig. 7C), despite its dating to 1740 BP. Broken Hill type ore, used previously in Australian petrol, has a very unradiogenic composition ($^{206}Pb/^{207}Pb = 1.04–1.10$) which explains the unique Pb isotope values in the surface sample (Gulson, 1986).

Lead three-isotope plots are used to trace dusts deposited at Lynch's Crater in Fig. 12. Data for peat samples, Group I and II and Cenozoic lavas from eastern Australia (Ewart et al., 1988; Zhang et al., 2001) is plotted as radiogenic ^{206}Pb, ^{207}Pb and ^{208}Pb normalised to the non-radiogenic ^{204}Pb. On the plot of $^{206}Pb/^{204}Pb$ vs. $^{208}Pb/^{204}Pb$ (Fig. 12A) the deposited dusts appear to be a simple mixture of Group I/Atherton basalts and Group II type rocks, with the former dominating. Soil samples demonstrate mixing between Group I/Atherton basalts and Group II as suggested by Eu anomaly data. Also similar to Eu anomaly data findings, the plot of $^{206}Pb/^{204}Pb$ vs. $^{207}Pb/^{204}Pb$ (Fig. 12B) evokes an unknown end-member contributing to the basal samples (905–1295 cm). Ewart et al. (1988) report no characteristic Pb isotope signatures exist among the volcanic provinces of eastern Australia except for the leucitite province in New South Wales where distinctly higher $^{207}Pb/^{204}Pb$ values were found. The mixing line for basal samples shown on the plot of $^{206}Pb/^{204}Pb$ vs. $^{207}Pb/^{204}Pb$ (Fig. 12B) indicates that the New South Wales leucitite province is a possible end-member. This corresponds with Eu anomaly source tracing results where basal samples are controlled by a long distance dust source.

5.3.4. Wet periods

The peat deposit is interspersed by four wet periods (P1–P4) whose samples are closely grouped near the basal sediment sample from 62.75 m on the Pb three isotope plots (Fig. 12A and B). The basal sediment reflects the catchment eroded during the initial lake stages in the crater which started some ~200,000 years ago (Kershaw, 1994). This similarity suggests that the material brought in during wet periods is also derived from erosion of the volcanic crater base. This is further confirmed by the fact that the basal sediment and P1–P4 samples fall into the Group I field, which represents the dominant local lithology on Pb three isotope plots. On the plot of $(La/Lu)_{PAAS}$ vs. $(Eu/Eu^*)_{PAAS}$ (Fig. 10) wet events also seem to include some inputs from Group II sources.

P2–P4 show sharp increases in REE concentrations on Al and Ti normalised profiles followed by decreases towards the end of the wet periods (Fig. 8A–F). The fine fraction in rocks and soils are major REE hosts and have higher REE concentrations than larger size fractions, related to the greater absorption of REE to clay minerals (McLennan, 1989; Minařík et al., 1998; Aubert et al., 2002; Yang et al., 2002; Compton et al., 2003; Gaiero et al., 2004; Caspari et al., in press). This increase in REE could indicate significant amounts of fine-grained materials, perhaps from extensive drying, were washed in during sudden shifts to wetter conditions. The tailing off of REE concentrations would indicate that clay minerals decreased in availability by the end of the wet period and/or that dilution of REE concentrations by quartz occurred (i.e., sand influx). This would also explain the HREE enrichment at the end of P1, P2 and P4 (Fig. 6A) as preferential fractionation of HREE into sand size fractions has been documented (Cullers et al., 1979; Cullers et al., 1987; Compton et al., 2003). SEM imaging found significant amounts of clay in P1 and P3 and rounded quartz grains ~50 μm in size in P2. Each wet event seems to differ in character and pre- and post effects of the increased sediment influx (Muller, 2006).

5.4. Paleoclimate: changes in dust deposition

5.4.1. Changepoint modelling

It is of primary interest to identify the timing and location of the distinct changes in dust source occurring at Lynch's Crater. We deal with a relatively noisy time (or depth) series however which makes this difficult. To solve this, the general Bayesian approach described by Denison et al. (2002) for dealing with such changepoint problems (or one-dimensional partition models) is used. In this it is

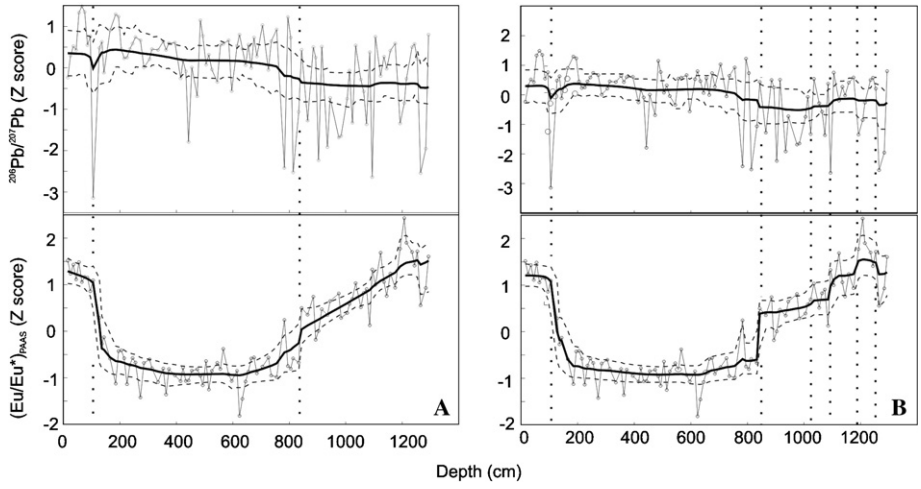

Fig. 13. Changepoint models for $(Eu/Eu^*)_{PAAS}$ and $^{206}Pb/^{207}Pb$ assuming both linear (A) and constant (B) regression functions. The posterior mean estimate (solid line) is the average of the predicted regression functions for both $(Eu/Eu^*)_{PAAS}$ and Pb isotope data. The 95% credible intervals around the predicted average curves for both types of regression functions are also given.

assumed that the underlying trends in the data between the changepoints are either constant or vary linearly with depth. These are estimated for a given number and location of changepoints by least squares regression for the data between each pair of changepoints. It is where the data imply they change, and not the underlying regression function that is of interest. As the changepoints here reflect different dust source contributions, Pb isotopes and $(Eu/Eu^*)_{PAAS}$ data were modelled simultaneously. In doing so, different regression functions for each data type are allowed for, but require that the changepoints be in the same location for each simulation considered. This Bayesian approach tends to favour simpler solutions (i.e., fewer changepoints). Numerous simulations were run with between 200,000 and 500,000 samples in each and the regression function within each partition was allowed to be either a constant value (i.e., one variable between each change point—the mean predicted value) or a linear function (i.e., two variables—between each change point—slope and intercept for the predicted values). A manuscript providing full details of this method is currently in preparation.

From this modelling a posterior mean estimate is generated and this is shown (see Denison et al., 2002, page 28) for both linear (Fig. 13A) and constant (Fig. 13B) regression function models. This mean is effectively the average over all sampled changepoint models of the predicted regression functions for both $(Eu/Eu^*)_{PAAS}$ and Pb isotope data. These average curves capture the most significant changepoints, as these will appear in many of the simulations while less important or poorly resolved changepoints tend to be smoothed out.

5.4.2. Identified changepoints and comparison with other records

Changepoint modelling (both linear and constant models) highlights two major changes in dust source at 38,930 BP (843.5 cm) and 8525 BP (105 cm). Smaller, less well-resolved changes (particularly on the constant regression model) in dust source occur between 43,640 and 51,220 BP (1023.5–1253.5 cm). Fig. 14 compares these changepoints with other records of paleoclimate, including: pollen records from Lynch's Crater (Kershaw, 1994) and Lake Wangoom in SE Australia (Edney, 1987, 1990); lake level records based on stratigraphy and geomorphological data from the Willandra Lakes in SE Australia (Bowler et al., 1976); and dune building activity in the interior of Australia based on ^{14}C and thermoluminescence dating (Wasson, 1986). Climate records from different regions show obvious

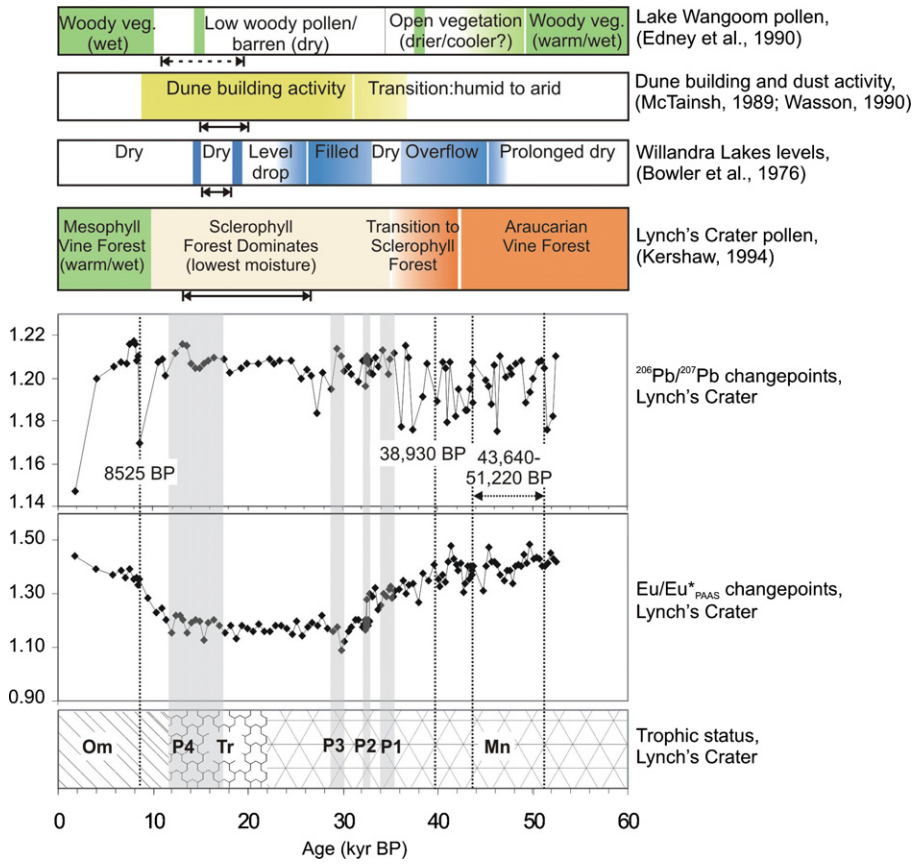

Fig. 14. The trophic status of the deposit and identified dust source changepoints are indicated on the age vs. $(Eu/Eu^*)_{PAAS}$ and $^{206}Pb/^{207}Pb$ profiles. This is compared with pollen reconstructions from Lynch's Crater and Lake Wangoom (located on the SE coast of Australia, not in Fig. 1), lake level records from Willandra Lakes and dune building records from the interior of Australia. Periods of maximum aridity are indicated under each record (arrows). Note the record from Lake Wangoom is discontinuous in this section.

variation e.g., vegetation changes at Lynch's Crater indicate dry conditions in NE Queensland while the Willandra Lakes in southern Australia were overflowing (Chappell, 1991), reflecting the asymmetry of climate changes in Australia.

Although varying by region and proxy type, a general drying trend in Australia starts 36–45 kyr BP. The pollen record from Lynch's Crater dates a shift to drier conditions between 35.5 and 42 kyr BP. During the transition from humid to arid conditions dust entrainment would be at its maximum. Changepoint modelling identifies the instant at which a change in the recorded dust source signal becomes statistically important. This transition to more arid conditions is reflected in the changepoint at 39 kyr BP but is obviously inset in a longer period of gradual change, noticeable on the $(Eu/Eu^*)_{PAAS}$ profile.

$(Eu/Eu^*)_{PAAS}$ reaches its lowest values and $^{206}Pb/^{207}Pb$ ratios show decreased variation (with the exception of during P4) during the period of maximum aridity in Australia between ~10 to 20 kyr BP. The abrupt change at 8.5 kyr BP coincides with changes in other proxies, including pollen from Lynch's Crater, and heralds the start of the warmer, wetter Holocene and local control of dust signatures.

The Willandra Lakes are located in the long distance range which was identified as an important dust source between 41,095 and 52,505 BP. The Willandra Lakes were dry from 120 to 45 kyr BP and then underwent a transition to overflowing lakes and rivers. With this transition reduced sediment, and consequently dust supply from the area would increase the importance of other dust sources (i.e., change from long distance to regional dust sources) and the small step changes between 44 and 51 kyr BP likely reflect this.

There is considerable agreement in the timing of dust source changepoints and vegetation/climate changes identified in the Lynch's Crater pollen record. Disparities between pollen and dust source records from Lynch's Crater likely reflect the broader geographical representation of the dust source record. The discussed records agree on the timing of maximum aridity and (with the exception of the Willandra Lakes record) the start of the Holocene in Australia. This includes our record of dust source changes, which confirms the application of REE and Pb isotopes as source tracers of atmospheric dusts and consequently, as proxies of climate change.

6. Conclusions

Using both elemental concentration and Pb isotope data analysed in a 13 m peat core collected from Lynch's Crater, NE Queensland, Australia this work explores REE behaviour in peats and developed REE and Pb isotopes as tools to identify changes in dust source. The identified changes in dust source are then interpreted in the context of climate change as recorded in eastern Australia over the last 52 kyr. From the data and discussion presented above the main conclusions are:

1. REE are immobile in the peat profile despite the organic rich and variable pH conditions in the mire. This is based on the high correlation between individual REE, the relatively unchanging REE patterns with depth and the grouping of REE with other known immobile elements in the first component of a PCA.
2. $(Eu/Eu^*)_{PAAS}$ is an effective dust source indicator where the geographical and chemical differences in the volcanic provinces of Australia are distinct enough to allow for the differentiation of their respective contributions.
3. Three phases of source dominance occurred during the last 52,505 years at Lynch's Crater:
   a. From 52,505 to 41,095 BP (905–1295 cm) long distance dust sources in New South Wales and Victoria dominate. This was identified using the high $(Eu/Eu^*)_{PAAS}$ values in the basal section of the core which must have contributions from evolved lavas; these are found only in regional (750–1500 km) and long distance (>1500 km) source areas. Contributions from long distance dust sources were further confirmed using the unique $^{207}Pb/^{204}Pb$ signature of the New South Wales leucitite province.
   b. From 40,815 to 8525 BP (105–895 cm) regional (100–1500 km) sources dominate the deposited signal as established using $(Eu/Eu^*)_{PAAS}$.
   c. In the upper part of the core, from 8390 to 1740 BP (5–95 cm) local sources contribute to the deposited signals. Samples from this part of the core fall into the local rock source fields on both $(Eu/Eu^*)_{PAAS}$ and Pb three isotope plots.
4. Changepoint modelling based on the dust source indicators $(Eu/Eu^*)_{PAAS}$ and $^{206}Pb/^{207}Pb$ identified significant changes in dust source occurred at 39 and 8.5 kyr BP. Minor changes are dated between 44 and 51 ky BP. In general, these changes agree with climate events reconstructed at Lynch's Crater using pollen. However, the dust source record integrates signals from a wider geographical area. REE and Pb isotopes provide a powerful method for source tracing atmospheric mineral dusts and are new proxies of climate change.

Acknowledgments

The authors express their gratitude to Sarah James, Gary Jones and Teresa Jeffries at the General Chemistry Lab and the Isoprobe users group at the Natural History Museum London for their support. Mike Warner, Andy Fleet and Terry Williams are also gratefully acknowledged. Professor Harry Elderfield and the Environmental Change and Marine Geochemistry group at the Department of Earth Sciences, Cambridge are thanked for providing a forum for fruitful discussion early in this project. Tony Ewart is thanked for his useful dialogue and generous data access. The help of Peter Kershaw is also much appreciated. Geraldine Jacobson

and Dennis Mather from the Australian Nuclear Sciences and Technology Organisation are thanked for their assistance with laboratory work. This work was made possible by financial support from the Australian Research Council (DP0451565) and the Australian Institute of Nuclear Sciences and Engineering (AINSTU0803), the Royal Society Imperial College London, the Natural History Museum London and Universities UK ORS Scholarship to MEK. The manuscript was improved by the helpful comments of three anonymous reviewers. MEK dedicates this article to MBA for all his love and support.

Associate editor: Martin Novak

Appendix A. Supplementary data

Supplementary data associated with this article can be found, in the online version, at doi:10.1016/j.gca.2006.10.018.

References

Akagi, T., Feng-Fu, F., Yabuki, S., 2002. Absence of Ce anomaly in the REE patterns of peat moss and peat grass in the Ozegahara peatland. *Geochem. J.* **36**, 113–118.

Aubert, D., Le Roux, G., Krachler, M., Cheburkin, A., Kober, B., Shotyk, W., Stille, P., 2006. Origin and fluxes of atmospheric REE entering an ombrotrophic peat bog in Black Forest (SW Germany): evidence from snow, lichens and mosses. *Geochim. Cosmochim. Acta* **70**, 2815–2826.

Aubert, D., Stille, P., Probst, A., Gauthier-Lafaye, F., Pourcelot, L., Del Nero, M., 2002. Characterization and migration of atmospheric REE in soils and surface waters. *Geochim. Cosmochim. Acta* **66**, 3339–3350.

Bau, M., 1991. Rare-earth element mobility during hydrothermal and metamorphic fluid-rock interaction and the significance of the oxidation state of europium. *Chem. Geol.* **93**, 219–230.

Bau, M., Usui, A., Pracejus, B., Mita, N., Kanai, Y., Irber, W., Dulski, P., 1998. Geochemistry of low-temperature water–rock interaction: evidence from natural waters, andesite, and iron-oxyhydroxide precipitates at Nishiki-numa iron-spring, Japan. *Chem. Geol.* **151**, 293–307.

Bindler, R., Klarqvist, M., Klaminder, J., Forster, J., 2004. Does within-bog spatial variability of mercury and lead constrain reconstructions of absolute deposition rates from single peat records? The example of Store Mosse, Sweden. *Global Biogeochem. Cycle* **18**, art. no.-GB3020.

Bowler, J.M., Hope, G.S., Jennings, J.N., Singh, G., Walker, D., 1976. Late quaternary climate changes of Australia and New Guinea. *Quat. Res.* **6**, 359–394.

Brännvall, M.L., Bindler, R., Emteryd, O., Nilsson, M., Renberg, I., 1997. Stable isotope and concentration records of atmospheric lead pollution in peat and lake sediments in Sweden. *Water Air Soil Pollut.* **100**, 243–252.

Braun, J.J., Pagel, M., Muller, J.P., Bilong, P., Michard, A., Guillet, B., 1993. Mobilization and redistribution of REEs and thorium in a syenitic lateritic profile: a mass balance study. *Geochem. Cosmochem. Acta* **57**, 4419–4434.

Caspari, T., Baumler, R., Norbu, C., Tshering, K., Baillie, I. (in press) Geochemical investigation of soils developed in different lithologies in Bhutan, Eastern Himalayas. Geoderma doi:10.1016/j.geoderma.2006.04.017.

Chappell, J., 1991. Late Quaternary environmental changes in eastern and central Australia, and their climatic interpretation. *Quat. Sci. Rev.* **10**, 377–390.

Compton, J.S., White, R.A., Smith, M., 2003. Rare earth element behaviour in soils and salt pan sediments of a semi-arid granitic terrain in the Western Cape, South Africa. *Chem. Geol.* **201**, 239–255.

Condie, K.C., 1991. Another look at rare earth elements in shales. *Geochim. Cosmochim. Acta* **55**, 2527–2531.

Cullers, R., Chaudhuri, S., Kilbane, N., Koch, R., 1979. Rare-earths in size fractions and sedimentary rocks of Pennsylvanian-Permian age from the mid-continent of the USA. *Geochim. Cosmochim. Acta* **43**, 1285–1301.

Cullers, R.L., Barrett, T., Carlson, R., Robinson, B., 1987. Rare-earths elements and mineralogic changes in Holocene soil and stream sediment: a case study in the Wet Mountains, Colorado, USA. *Chem. Geol.* **63**, 275–297.

Denison, D., Holmes, C., Mallick, B., Smith, A., 2002. *Bayesian Methods for Nonlinear Classification and Regression*. Wiley, New York.

Dia, A., Gruau, G., Olivie-Lauquet, G., Riou, C., Molénat, J., Curmi, P., 2000. The distribution of rare earth elements in groundwaters: assessing the role of source-rock composition, redox changes and colloidal particles. *Geochim. Cosmochim. Acta* **64**, 4131–4151.

Edney, P.A., 1987. Late Quaternary vegetation and environments from Lake Wangoom, western Victoria, Unpublished Masters Thesis, Monash University.

Edney, P.A., Kershaw, P., De Deckker, P., 1990. A Late Pleistocene and Holocene vegetation and environmental record from Lake Wangoom, Western Plains, Victoria. *Paleogeogr. Paleoclimatol. Paleoecol.* **80**, 325–343.

Elderfield, H., Upstill-Goddard, R., Sholkovitz, E.R., 1990. The rare-earth elements in rivers, estuaries, and coastal seas and their significance to the composition of ocean waters. *Geochim. Cosmochim. Acta* **54**, 971–991.

Ewart, A., Chappell, B.W., Menzies, M.A., 1988. An overview of the geochemical and isotopic characteristics of the Eastern Australian Cainozoic Volcanic Provinces. *J. Petrol. Spec. Lithosphere Issue*, 225–273.

Fink, d., Hotchkis, M., Hua, Q., Jacobsen, G., Smith, A.M., Zoppi, U., Child, D., Mifsud, C., Van DerGaast, H., Williams, A., Williams, M., 2004. The ANTARES AMS facility at ANTSO. *Nucl. Instrum. Methods B* **223–224**, 109–114.

Gaiero, D.M., Depetris, P.J., Probst, J.-L., Bidart, S.M., Leleyter, L., 2004. The signature of river- and wind-borne materials exported from Patagonia to the southern latitudes: a view from REEs and implications for paleoclimatic interpretations. *Earth Planet. Sci. Lett.* **219**, 357–376.

Galer, S.J.G., Abouchami, W., 1998. Practical application of lead triple spiking for correction of instrumental mass discrimination. *Miner. Mag.* **62A**, 205–215.

Gallet, S., Jahn, B.-m., Torii, M., 1996. Geochemical characterization of the Luochuan loess-paleosol sequence, China, and paleoclimatic implications. *Chem. Geol.* **133**, 67–88.

Gallet, S., Jahn, B.-m., Van Vliet Lanoe, B., Dia, A., Rossello, E., 1998. Loess geochemistry and its implications for particle origin and composition of the upper continental crust. *Earth Planet. Sci. Lett.* **156**, 157–172.

Ganor, J., Roueff, E., Erel, Y., Blum, J.D., 2005. The dissolution kenetics of a granite and its minerals-Implications for comparison between labratory and field dissolution rates. *Geochim. Cosmochim. Acta* **69**, 607–621.

Gulson, B.L., 1986. *Lead Isotopes in Mineral Exploration*. Elsevier, Amsterdam.

Hannigan, R.E., Sholkovitz, E.R., 2001. The development of middle rare earth element enrichments in freshwaters: weathering of phosphate minerals. *Chem. Geol.* **175**, 495–508.

Harlavan, Y., Erel, Y., 2002. The release of Pb and REE from granitoids by the dissolution of accessory phases. *Geochim. Cosmochim. Acta* **66**, 837–848.

Hodson, M.E., 2002. Experimental evidence for mobility of Zr and other trace elements in soils. *Geochim. Cosmochim. Acta* **66**, 819–828.

Ji, H., Wang, S., Ouyang, Z., Zhang, S., Sun, C., Liu, X., Zhou, D., 2004. Geochemistry of red residua underlying dolomites in karst terrains of Yunnan-Guizhou Plateau: II. The mobility of rare earth elements during weathering. *Chem. Geol.* **203**, 29–50.

Johannesson, K.H., Tang, J., Daniels, J.M., Bounds, W.J., Burdige, D.J., 2004. Rare earth element concentrations and speciation in organic-rich blackwaters of the Great Dismal Swamp, Virginia, USA. *Chem. Geol.* **209**, 271–294.

Kamber, B.S., Greig, A., Collerson, K.D., 2005. A new estimate for the composition of weathered young upper continental crust from alluvial sediments, Queensland, Australia. *Geochim. Cosmochim. Acta* **69**, 1041–1058.

Kershaw, P., 1974. A long continuous pollen sequence from north-eastern Australia. *Nature* **251**, 222–223.

Kershaw, P., 1994. Pleistocene vegetation of the humid tropics of northeastern Queensland, Australia. *Paleogeogr. Paleoclimatol. Paleoecol.* **109**, 399–412.

Klaminder, J., Renberg, I., Bindler, R., Emteryd, O., 2003. Isotopic trends and background fluxes of atmospheric lead in northern Europe: analyses of three ombrotrophic bogs from south Sweden. *Global Biogeochem. Cycle* **17**, 1019–1028.

Kohfeld, K.E., Harrison, S.P., 2001. DIRTMAP: the geological record of dust. *Earth-Sci. Rev.* **54**, 91–114.

Krachler, M., Mohl, C., Emons, H., Shotyk, W., 2003. Two thousand years of atmospheric rare earth element (REE) deposition as revealed by an ombrotrophic peat bog profile, Jura Mountains, Switzerland. *J. Environ. Monit.* **5**, 111–121.

Kylander, M., Weiss, D., Martinez Cortizas, A., Spiro, B., Garcia Sanchez, R., Coles, B.J., 2005. Refining the pre-industrial atmospheric lead isotope evolution curve in Europe using an 8,000 years old peat core from NW Spain. *Earth Planet. Sci. Lett.* **240**, 467–485.

Kylander, M.E., Weiss, D.J., Jeffries, T., Coles, B.J., 2004. Sample preparation procedures for accurate and precise isotope analysis of Pb in peat by multiple collector (MC)-ICP-MS. *J. Anal. At. Spectrom.* **19**, 1275–1277.

Land, M., Ohlander, B., Ingri, J., Thunberg, J., 1999. Solid speciation and fractionation of rare earth elements in a spodosol profile from northern Sweden as revealed by sequential extraction. *Chem. Geol.* **160**, 121–138.

Le Roux, G., Laverret, E., Shotyk, W., 2006. Fate of calcite, apatite and felspars in an ombrotrophic peat bogs, Black Forest, Germany. *J. Geol. Soc. Lond.* **163**, 641–646.

Lee, J., Tallis, J., 1973. Regional and historical aspects of lead pollution in Britain. *Nature* **245**, 216–220.

Martínez Cortizas, A., Pontevedra Pombal, X., García-Rodeja Gayoso, E., Nóvoa Muñoz, J.C., Shotyk, W., 1999. Mercury in a Spanish peat bog: archive of climate change and atmospheric metal deposition. *Science* **284**, 939–942.

Marx, S.K., Kamber, B.S., McGowan, H.A., 2005a. Estimates of Australian dust flux into New Zealand: Quantifying the eastern Australian dust plume pathway using trace element calibrated 210Pb as a monitor. *Earth Planet. Sci. Lett.* **239**, 336–351.

Marx, S.K., Kamber, B.S., McGowan, H.A., 2005b. Provenance of long-travelled dust determined with ultra-trace-element composition: a pilot study with samples from New Zealand glaciers. *Earth Surf. Processes Landf.* **30**, 699–716.

McLennan, S.M., 1989. Rare earth elements in sedimentary rocks: influence of provenance and sedimentary processes. In: Lipin, B.R., McKay, G.A. (Eds.), *Geochemistry and Mineralogy of Rare Earth Elements*, vol. 21. Mineralogical Society of America, pp. 169–200.

McTainsh, G.H., 1989. Quaternary aeolian processes and sediments in the Australian region. *Quat. Sci. Rev.* **8**, 235–253.

Minařík, L., Žigová, A., Bendl, J., Skřivan, P., Šťastný, M., 1998. The behaviour of rare-earth elements and Y during the rock weathering and soil formation in the Ricany granite massif, Central Bohemia. *Sci. Total Environ.* **215**, 101–111.

Möller, P., 2002. Rare earth elements and yttrium distribution in water–rock interactions: field observations and experiments. In: Bucher, K. (Ed.), *Water–Rock Interactions*. Kluwer Academic Publishers, pp. 97–123.

Möller, P., Dulski, P., Gerstenberger, H., Morteani, G., Fuganti, A., 1998. Rare earth elements, yttrium and H, O, C, Sr, Nd and Pb isotope studies in mineral waters and corresponding rocks from NW-Bohemia, Czech Republic. *Appl. Geochem.* **13**, 975–994.

Möller, P., Irber, W., Giese, U., 1997. Determination of easily accessible metals fractions in rocks by batch leaching with acid cation exchange resin. *Chem. Geol.* **137**, 41–55.

Muller, J., 2006. *Reconstructing Climate Change of the Last 55 kyr: The Lynch's Crater Peat Mire Record*. James Cook University, NE-QLD, Australia.

Muller, J., Wüst, R.A.J., Weiss, D.J., Hu, Y., 2006. Geochemical and stratigraphic evidence of environmental change at Lynch's Crater, Queensland, Australia. *Global Planet. Change* **53**, 269–277.

Nesbitt, H.W., 1979. Mobility and fractionation of REE during weathering of granodiorite. *Nature* **279**, 206–210.

Pearce, B., 2002. Report on compilation of a geological conceptual model for the Atherton Tableland Basalts. Queensland Department of Natural Resources and Mines.

Price, R.C., Gray, C.M., Wilson, R.E., Frey, F.A., Taylor, S.R., 1991. The effects of weathering on rare-earth element, Y and Ba abundances in Tertiarybasalts from southeastern Australia. *Chem. Geol.* **93**, 245–265.

Rea, D.K., 1994. The paleoclimatic record provided by eolian deposition in the deep sea: the geologic history of wind. *Rev. Geophys.* **32**, 159–195.

Rosman, K.J.R., Chisholm, W., Hong, S., Candelone, J.P., Boutron, C.F., 1997. Lead from Carthaginian and Roman Spanish mines isotopically identified in Greenland ice dated from 600 BC to 300 AD. *Environ. Sci. Technol.* **31**, 3413–3416.

Roy, P.D., Smykatz-Kloss, W., in press. REE geochemistry of the recent playa sediments from the Thar Desert, India: an implication to playa sediment provenance. *Chem. Erde* doi:10.1016/j.chemer.2006.01.006.

Sholkovitz, E.R., 1992. Chemical evolution of rare-earth elements: fractionation between colloidal and solution phases of filtered river water. *Earth Planet. Sci. Lett.* **114**, 77–84.

Shotyk, W., Goodsite, M.E., Roos-Barraclough, F., Frei, R., Heinemeier, J., Asmund, G., Lohse, C., Hansen, T.S., 2003. Anthropogenic contributions to atmospheric Hg, Pb and As accumulation recorded by peat cores from southern Greenland and Denmark dated using the ^{14}C "bomb pulse curve". *Geochim. Cosmochim. Acta* **67**, 3991–4011.

Shotyk, W., Goodsite, M.E., Roos-Barraclough, F., Givelet, N., Le Roux, G., Weiss, D., Cheburkin, A.K., Knudsen, K., Heinemeier, J., van Der Knaap, W.O., 2005. Accumulation rates and predominant atmospheric sources of natural and anthropogenic Hg and Pb on the Faroe Islands. *Geochim. Cosmochim. Acta* **69**, 1–17.

Shotyk, W., Weiss, D., Kramers, J.D., Frei, R., Cheburkin, A.K., Gloor, M., Reese, S., 2001. Geochemistry of the peat bog at Etang de la Gruère, Jura Mountains, Switzerland, and its record of atmospheric Pb and lithogenic trace metals (Sc, Ti, Y, Zr, and REE) since 12,370 ^{14}C yr BP. *Geochim. Cosmochim. Acta* **65**, 2337–2360.

Steinmann, P., Shotyk, W., 1997. Geochemistry, mineralogy, and geochemical mass balance on major elements in two peat bog profiles (Jura Mountains, Switzerland). *Chem. Geol.* **138**, 25–53.

Stephenson, P.J., Griffin, T.J., Sutherland, F.L., 1980. *Cainozoic Volcanism in North-Eastern Australia*. Geological Society of Australia, Brisbane.

Taylor, S.R., McLennan, S.M., 1985. *The Continental Crust: Its Composition and Evolution*. Blackwell, Oxford.

Tolonen, K., 1984. Interpretation of changes in the ash content of ombrotrophic peat layers. *Bull. Geol. Soc. Finland* **56**, 207–219.

Turney, C.S.M., Kershaw, P., Clemens, S.C., Branch, N., Moss, P., Fifield, L.K., 2004. Millennial and orbital variations of El Nino/Southern Oscillation and high-latitude climate in the last glacial period. *Nature* **428**, 306–310.

Warneck, P., 2000. *Chemistry of the Natural Atmosphere*. Academic Press, London.

Wasson, R.J., 1986. Geomorphology and Quaternary history of the Australian continental dunefields. *Geogr. Rev. Jpn.* **59**, 55–67.

Weber, E.T.I., Owen, R.M., Dickens, G.R., Rea, D.K., 1998. Causes and implications of the middle rare earth element depletion in the eolian component of North Pacific sediment. *Geochim. Cosmochim. Acta* **62**, 1735–1744.

Wedepohl, K.H., 1995. The composition of the continental-crust. *Geochim. Cosmochim. Acta* **59**, 1217–1232.

Weiss, D., Shotyk, W., Rieley, J., Page, S., Gloor, M., Reese, S., Martínez Cortizas, A., 2002. The geochemistry of major and selected trace elements in a forested peat bog, Kalimantan, SE Asia, and its implications for past atmospheric dust deposition. *Geochim. Cosmochim. Acta* **66**, 2307–2323.

Weiss, D.J., Kober, B., Dalgopolova, A., Gallagher, K., Spiro, B., Le Roux, G., Mason, T.F.D., Kylander, M.E., Coles, B.J., 2004. Accurate and precise Pb isotope ratio measurements in environmental samples by MC-ICP-MS. *Int. J. Mass Spectrom.* **232**, 205–215.

Weiss, D.J., Shotyk, W., Appleby, P.G., Kramers, J.D., Cheburkin, A., 1999. Atmospheric Pb deposition since the Industrial Revolution recorded by five Swiss peat profiles: enrichment factors, fluxes, isotopic composition, and sources. *Environ. Sci. Technol.* **33**, 1340–1352.

Wilson, M., 2000. *Igneous Petrogenesis: A Global Tectonic Approach*. Kluwer Academic Publishers, London.

Yang, S.Y., Jung, H.S., Choi, M.S., Li, C.X., 2002. The rare earth element compositions of the Changjiang (Yangtze) and Huanghe (Yellow) river sediments. *Earth Planet. Sci. Lett.* **201**, 407–419.

Yang, S.Y., Lim, D.I., Jung, H.S., Oh, B.C., 2004. Geochemical composition and provenance discrimination of coastal sediments around Cheju Island in the southeastern Yellow Sea. *Mar. Geol.* **206**, 41–53.

Ylirukanen, I., Lehto, S., 1995. The occurrence of rare earth elements in some Finnish mires. *Bull. Geol. Soc. Finland*, 27–38.

Zhang, M., Stephenson, P.J., O'Reilley, S.Y., McCulloch, M., Norman, M., 2001. Petrogenesis and geodynamic implications of late Cenozoic basalts in North Queensland, Australia: trace-element an d Sr-Nd-Pb isotope evidence. *J. Petrol.* **42**, 685–719.